PERGAMON

Quaternary Science Reviews 21 (2002) 709–731

QSR

Holocene history of the Great Kobuk Sand Dunes, Northwestern Alaska

D.H. Mann[a,*], P.A. Heiser[b], B.P. Finney[c]

[a] *Institute of Arctic Biology, Irving I Building, University of Alaska, Fairbanks, AK 99775, USA*
[b] *Department of Geology, 316 Clippinger Laboratories, Ohio University, Athens, OH 45701, USA*
[c] *Institute of Marine Science, Irving II Building, University of Alaska, Fairbanks, AK 99775, USA*

Abstract

Located just north of the Arctic Circle, the Great Kobuk Sand Dunes (GKSD) are an inland dune field that is closely surrounded by boreal forest. The history of the GKSD tells us about changes in aridity, a climatic parameter whose history is poorly understood at high latitudes. Vegetated dunes in several states of geomorphic preservation surround the active dune field today, evidencing a complex history of Holocene activity. Small lakes in the forest bordering the dunes accumulate wind-blown sand. We use ^{14}C-dated, lake-sediment cores to reconstruct a continuous history of sand influx over the last 8000 yr. The validity of this record is supported by limiting ages obtained from stratigraphic sections within the dune field. The extent of the GKSD underwent a fluctuating shrinkage coincident with Neoglaciation. This downsizing trend was interrupted by periods of increased sand deposition into lakes occurring 4800–4200, 3300–2600, 1300–700, and 300–100 calendar years ago. Aridity in the Kobuk valley during the Holocene probably was controlled by the frequency of North Pacific storms entering the region in late summer. Our results describe the first continuous history of changing moisture balance for central Beringia during the Holocene and comprise a baseline against which future records of climatic and ecological change in this region can be compared. © 2002 Elsevier Science Ltd. All rights reserved.

1. Introduction

During the last glacial period, sand sheets and dunes covered $>30{,}000\,km^2$ in northern Alaska (Carter, 1981; Hopkins, 1982; Lea and Waythomas, 1990). Today, aeolian processes are of minor importance in the taiga and tundra landscapes of this region. Only two large, active dune fields survive in areas distant from the coast: the Great Kobuk Sand Dunes (GKSD) in the central Kobuk valley and the Nogahabara Dunes (Koster et al., 1984) in the lower Koyukuk valley (Fig. 1). Here, we describe changes in the extent and activity of the GKSD during the mid- and late Holocene.

The Holocene dynamics of the Great Kobuk Sand Dunes are of interest for several reasons. This dune field's history and future are important for the conservation of rare plant species that are native to these dunes (Young and Racine, 1977). Also, the GKSD are part of the subsistence landscape utilized by the Inupiat people of the Kobuk valley, and the dune field's history is potentially important for archaeological record (Anderson, 1988a). Finally, remnant dune fields existing as islands within a sea of boreal forest vegetation are likely to be poised at climatic thresholds and hence be sensitive indicators of climatic change. Our objectives here are to reconstruct the Holocene history of the GKSD and to infer its climatic causes.

This study relies on three complimentary sources of data: stratigraphic sections exposed in stream cuts and soil pits, the ages of trees buried by dunes, and sediment cores from dune-marginal lakes. We began this project by studying outcrops exposed in stream cuts and soil pits and by ^{14}C-dating trees exhumed in interdune swales. However, sand dunes leave only discontinuous stratigraphic records within the boundaries of dune fields. It became obvious that we needed a more complete proxy record of dune-field activity, which we found in the continuously deposited sediments of a dune-marginal lake. But was the influx of sand into a single lake representative of the activity of the entire dune field? To answer this question, we use the terrestrial stratigraphy to test the validity of the lake-core record. Once validated, the lacustrine

*Corresponding author. Tel.: 1-907-455-6249.
E-mail address: dmann@mosquitonet.com (D.H. Mann).

0277-3791/02/$ - see front matter © 2002 Elsevier Science Ltd. All rights reserved.
PII: S0277-3791(01)00120-2

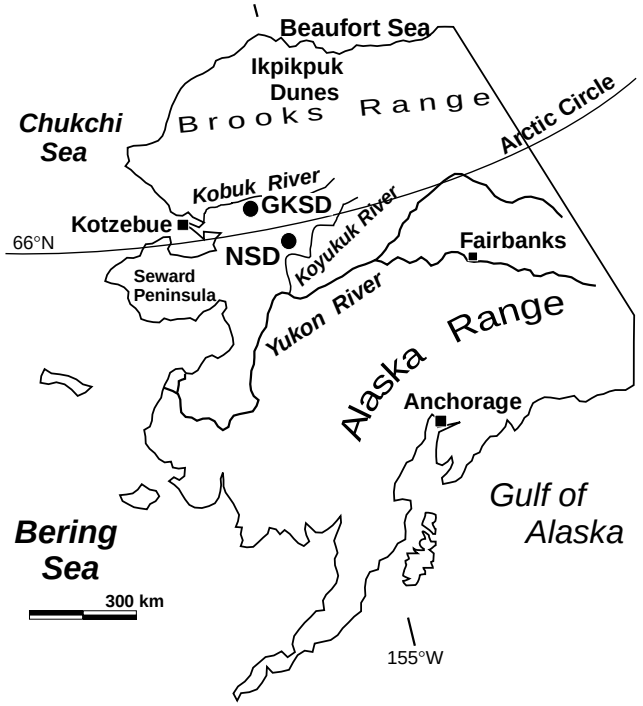

Fig. 1. Alaska with locations of sites mentioned in text along with other key physiographic features. The only other, large active dune field in interior Alaska is the Nogahabara (NSD). The IKpikpuk dune field is presently active.

record provides a closely dated proxy for dune-field activity.

2. Previous studies

The morphology and sedimentology of the GKSD have been studied extensively as analogs for prehistoric, cold-climate aeolian systems (Dijkmans et al., 1986, 1988; Koster and Dijkmans, 1988; Dijkmans and Koster, 1990), but no previous studies address the Holocene history of this dune field. Mapping of surficial geology revealed that the Kobuk dunes were previously much more extensive (Fernald, 1964; Hamilton, 1984; Kuhry-Helmens et al., 1985). Vegetated dune forms in several different states of geomorphic modification (fresh, sharp-crested dunes versus smooth, low-relief features) surround the active dune field and suggest that major fluctuations in aeolian activity occurred during the Holocene.

A long history of aeolian activity in the Kobuk valley is recorded by interbedded fluvial sediments, terrestrial peats, and aeolian sediments exposed in a spectacular cutbank section at Epiguruk, 25 km northeast of the GKSD (Fig. 2) (Ashley and Hamilton, 1993). Pleistocene glaciation of the Brooks Range was accompanied by alluviation and aeolian activity in the Kobuk valley. During the last glacial maximum, 24,000–19,000 ^{14}C yr BP, the greatly expanded Kobuk dunes filled the middle reaches of the Kobuk valley (Hamilton et al., 1987). The Kobuk River was overloaded with sandy sediment and alluviated some 13 m above its present level at Epiguruk (Hamilton and Ashley, 1993). Downcutting by the river and shrinkage of the dune field occurred after 18,500 ^{14}C yr BP. By 8600 ^{14}C yr BP, the river had established a floodplain near its modern level. Peat deposition started at Epiguruk ca. 3600 ^{14}C yr BP (Hamilton and Ashley, 1993), implying a significant increase in effective moisture (precipitation–evapotranspiration).

Palynological research in northwest Alaska by Anderson (1985,1988b) documented several changes in vegetation during the Holocene that probably resulted from climatic shifts. Following tundra during the last glacial period, alder (*Alnus*) arrived in the area ca. 9000 ^{14}C yr BP in response to the advent of a warmer and more moist climate. Spruce (*Picea*), probably mostly black spruce (*P. mariana*), arrived in the Kobuk valley 5000–6000 ^{14}C yr BP, perhaps in response to a further increase in moisture. The present forest–tundra vegetation mosaic likely dates to that time. Pollen records from arctic vegetation are notoriously insensitive to climate change (Anderson et al., 1994), and numerous climatic fluctuations may be unrecorded by the existing pollen records.

Glacier fluctuations in the Brooks Range (Ellis and Calkin, 1984; Calkin, 1988) and on the Seward Peninsula (Calkin et al., 1998), together with intermittent construction of beach ridges in the Chukchi Sea (Mason and Jordan, 1993; Mason et al., 1995), document repeated climatic fluctuations during the late Holocene in northwestern Alaska. Interpretation of the beach-ridge record in terms of paleoclimate is difficult because of the complexity of stratigraphic and climatic arguments. The glacial record, based mainly on lichenometry, suggests advances ca. 4500, 3500, 2800, and perhaps 2000 ^{14}C yr BP (Ellis and Calkin, 1984). A series of closely spaced glacier advances began ca. AD 800 and continued into the 19th century. The relative shortness ($\sim$400 yr) of tree-ring records from northern Alaska (D'Arrigo and Jacoby, 1995; Jacoby et al., 1999) and their interpretation in terms of temperature history make comparisons with the GKSD record difficult. These other proxy records of climatic change, although still fragmentary, indicate considerable climate variability during the Holocene in northwestern Alaska.

3. Study area

3.1. Geography and landforms

An area of 650 km^2 in the middle reaches of the Kobuk valley is underlain by sand that was affected episodically by aeolian activity over the last 10^4 yr (Fernald, 1964; Hamilton, 1984; Hamilton et al., 1987).

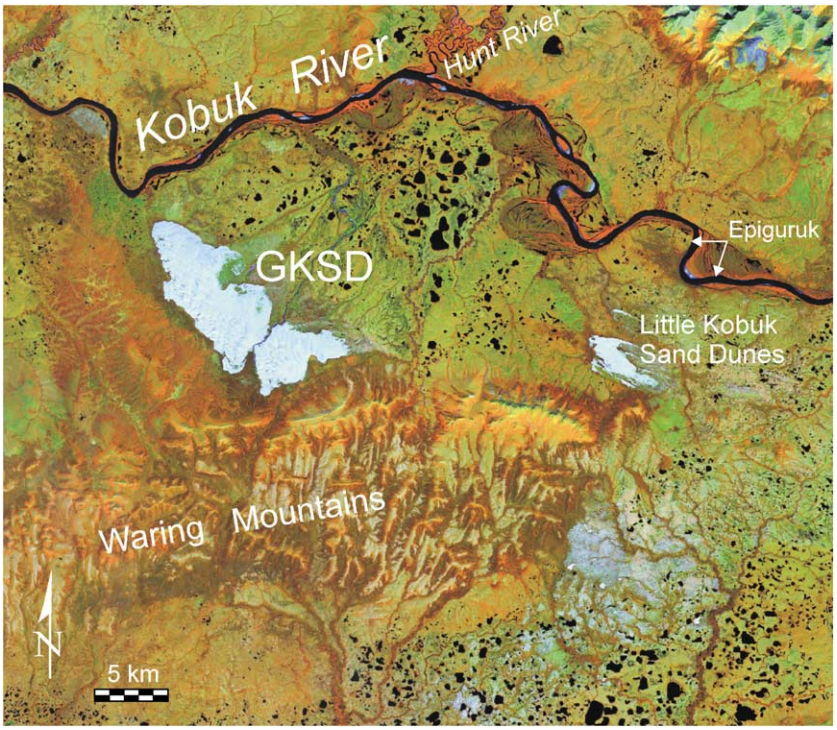

Fig. 2. False color satellite image of the Kobuk valley showing areas of active and inactive sand dunes. Landsat Thematic Mapper mosaic from path 78, row 13 acquired on 6 July, 1985. Image courtesy of US National Park Service, Alaska Support Office, GIS Landcover Mapping Program, Anchorage, AK.

Today, only three areas of active dunes and sand sheets exist within this Pleistocene sand fill (Fig. 2). Active dunes occur for several kilometers along the Kobuk River near the mouth of Hunt River (Hamilton et al., 1987). The Little Kobuk Dunes (8 km^2) are an elongate patch of blowouts and parabolic dunes with barchanoid dunes at their western extremity (Kuhry-Helmens et al., 1985). The Great Kobuk Dunes (62 km^2) are the largest active dune fields in the area and contain a diverse assemblage of aeolian landforms including parabolic, transverse, longitudinal, and barchanoid dunes, along with sand sheets, nabkhas, blowouts, and precipitation ridges (Koster and Dijkmans, 1988; Dijkmans and Koster, 1990). Precipitation ridges, or *randwallen*, develop where forests bordering active dunes cause wind speed to drop. Sand is deposited along a linear crest above a slipface that advances into the adjacent forest (Cooper, 1967; Raup and Argus, 1982). Precipitation ridges from much of the perimeter of the GKSD today.

The GKSD lie in a 20 km long, topographic amphitheater facing NNE, which is formed by flanking ridges of the low (200–600 m) Waring Mountains (Fig. 2). The southwestern margin of the GKSD has climbed onto the lower slopes of this topographic barrier to altitudes of 160 m, though most of the active dune field lies at altitudes of 60–80 m above sea level. Three streams drain the northern slopes of the Waring Mountains and interact with the GKSD. Their alluvial histories provide proxy records for dune-field activity. When the dunes are active, blowing sand overwhelms the sediment-transporting capacities of these streams. Stream courses are diverted upslope by advancing dunes, and floodplains aggrade. When the dunes are less active, streams downcut rapidly through the sandy valley fills. The active dune field presently diverts Niaktuvik and Kavet Creeks to the dune-field margin (Fig. 3). In their upper reaches, both these streams probably lose part of their flow to infiltration into the adjacent dune field. Ahnewetut Creek maintains its course across the GKSD despite large quantities of sand blown in and across it during winter.

3.2. Dune dynamics and sand characteristics

Net sand drift in the GKSD, as indicated by dune orientations, is primarily to the west and northwest, though summer winds cause minor eastward drift. The ultimate source for the sand composing the GKSD is quartzose bedrock in the Brooks Range that was eroded and transported by glaciers and outwash streams into the Kobuk valley during Pleistocene glaciations (Hamilton, 1984). Today, there is no sand source for the GKSD other than the underlying, older sandy sediments. At present, the GKSD are separated from the sandy floodplain of the Kobuk River by 3–20 km of dense vegetation.

Despite being cut off from fluvial sources of sand today, the limiting factor in the GKSD seems to be

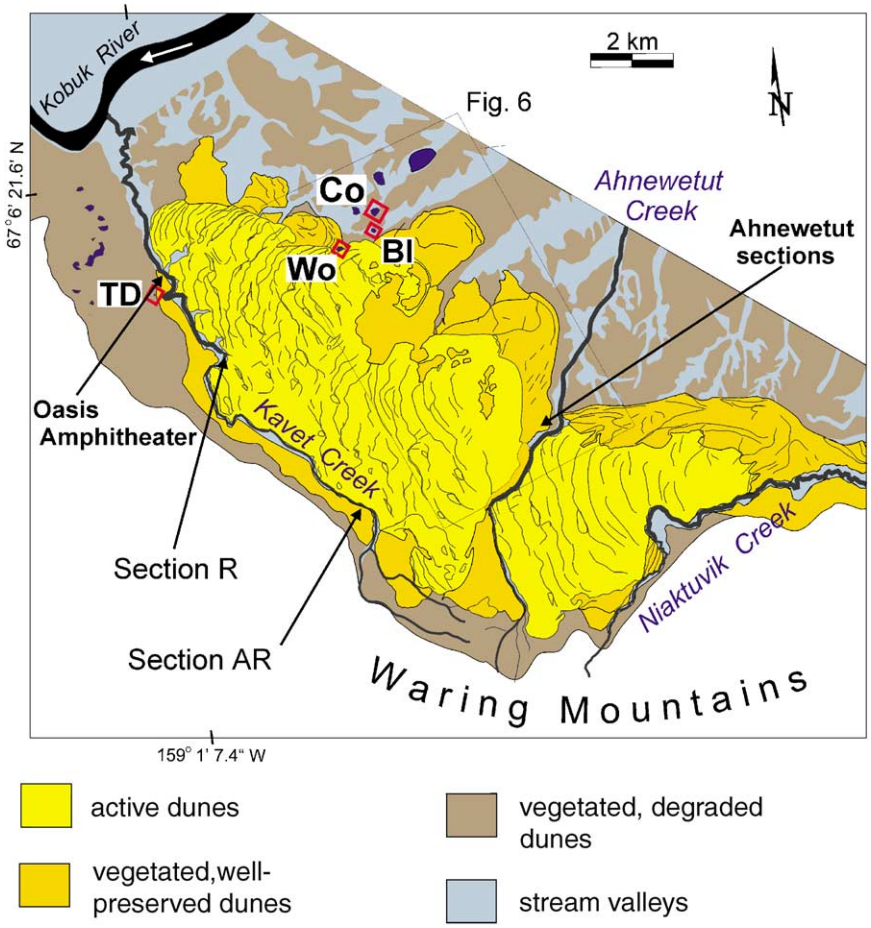

Fig. 3. GKSD showing areas of active, recently active, and long-inactive sand dunes. Based on interpretation of 1:60,000 color infrared aerial photography and ground truthing. "TD" is Thigh Deep Pond. "Wo" is Lake Wolverine. "Bl" is Black Lake. "Co" is Cow Lake. All are informal names.

sediment availability, not sediment supply (cf., Kocurek and Lancaster, 1999). Holocene-dune building is the result of reworking of the Pleistocene sand deposits (cf., Lea and Waythomas, 1990) that underlie the modern dune field. At Epiguruk, the sandy valley fill is >30 m thick (Hamilton and Ashley, 1993). Forty meters of subhorizontally stratified, aeolian sands are exposed under a forest cover along the bank of the Kobuk River several kilometers downstream of Kavet Creek (Fig. 3). We infer that the availability of these underlying sands for dune and sand sheet growth depends on the interrelated factors of soil moisture and vegetation cover.

Sands in the GKSD are fine-grained with a mean diameter of 170 μm, and are moderately well sorted, symmetrical, and meso- to leptokurtic (Dijkmans et al., 1988). Grain counts sand samples (Dijkmans et al.,1986) show that quartz and feldspar are the dominant minerals (78%), accompanied by heavy minerals (10%), and carbonate (7%). Phyllosilicate minerals, garnet, epidote, amphibole, and chloritoid are minor components. Carbonate grains in the dune sands are a mixture of detrital grains derived from bedrock and calcite precipitated as secondary carbonates within the dune field. In 20 samples of aeolian sand, Dijkmans et al. (1986) found weight percentages of carbonate ranging from 1% to 4%. The mean $CaCO_3$ content of 25 samples of aeolian sand that we collected was 1.5% (SE = 0.15), as determined by weight loss on heating. Secondary carbonates are widespread in the GKSD where they precipitate in frost cracks, around springs, and in interdune basins (Cox and Lawrence, 1983; Koster et al., 1986; Galloway et al., 1990). Isotopic analysis suggests that calcretes are formed in the GKSD primarily by the exposure of cold, carbonate-rich groundwater to warm surface conditions with lower partial pressures of CO_2 (Dijkmans et al., 1986).

3.3. Vegetation

The GKSD are surrounded closely by boreal forest (Racine, 1976). On well-drained sites within 50–100 m of the active dunes, this forest is dominated by 10–20 m tall white spruce (*Picea glauca*) with subordinate birch (*Betula papyrifera*) and aspen (*Populus tremuloides*). Farther from the active dunes, well-drained, stabilized

dunes are covered by forest parklands of white spruce, birch, aspen, willow (*Salix* species), and alder (*Alnus crispa*), with a ground layer of ericaceous shrubs (Ericaceae) and foliose lichens (Young and Racine, 1977). Black spruce (*P. mariana*) dominates poorly drained sites together with feather mosses (genera *Pleurozium* and *Hylocomium*), sphagnum mosses (*Sphagnum* spp.), and ericaceous shrubs. Sand-sheet areas along the eastern margin of the dune field support sparse vegetation dominated by grasses and perennial herbs.

3.4. Climate

The GKSD have a moderately continental, subarctic climate with long, cold winters and brief, warm summers. In the middle and upper Kobuk valley, mean annual temperature is –6°C, and mean July temperatures is 15°C (Leslie, 1989; PRISM, 2000). Mean annual precipitation ranges from 300 to 500 mm along the southern slopes of the western Brooks Range (Hartman and Johnson, 1984; PRISM, 2000). Almost two-thirds of the annual precipitation falls as rain between July and October, primarily during the passage of storms entering the region from the North Pacific (Hare and Hay, 1974; Moritz, 1979; Mock et al., 1998). The Kobuk valley has a droughty climate for plant growth. Moisture deficits (potential evapotranspiration–actual evapotranspiration) range from 10 to 140 mm yr^{-1} in this region (Patric and Black, 1968; Newman and Branton, 1972).

Winter (December–March) is the windiest season, and summer is the calmest, with autumn and spring transitional between the two. Wind speed averages 6 m s^{-1} in winter in the Kobuk valley (DeHarpporte, 1983). Easterly winds in winter blow snow off the active dunes, leaving the sand exposed to wind action (Koster and Dijkmans, 1988). During summer, winds are weaker and more variable, with southerly and westerly winds prevailing (Dijkmans and Koster, 1990).

3.5. Permafrost

Although the Kobuk valley is believed to lie within the zone of continuous permafrost (Ferrians, 1994), we found no frozen ground within several meters of the surface at many localities. We tested five sites within the active dunes (two dune crests, three interdune areas) with a soil auger in September 1997 and found no permafrost within 4 m of the surface. Soil pits on the crests and southern flanks of now-forested dunes showed no evidence of permafrost within 1 m of the ground surface. At two south-facing sites in Holocene-aged, now-forested dunes, we dug to 2 m in late September 1996 without striking permafrost. In contrast, north-facing slopes with thick ground covers of moss and overstories of conifer trees had permafrost within 1 m of the surface. Thaw lakes are abundant on the sand plain east of the GKSD. West of the active dunes, another area of stabilized dunes also contains numerous thaw ponds (Fig. 2). Permafrost may be present at depth beneath the GKSD, but it approaches the surface only in vegetated areas around their periphery.

4. Part I: Stratigraphic sections and buried forests

4.1. Methods and modern facies associations

We worked in the GKSD in late summer when the ground was deeply thawed. We dug soil pits at the distal toe slopes of precipitation ridges to expose buried soils and cleared cut-bank sections over the course of several days' digging at each site. We also collected wood and bark from the outer surfaces of tree trunks and stumps exposed in interdune swales.

We described and interpreted stratigraphic sections exposed in stream cuts and soil pits using the facies associations present in and around the modern dune field. Small-scale sets (<10 cm) of trough cross-laminae formed by linguoid ripples of medium to very fine sand are diagnostic of the deposits left by the shallow, braided streams flowing through or alongside the dunes (Ashley and Hamilton, 1993). In section, microtrough sets often are cut by channel-scour surfaces overlain by massive or planar bedded sands containing granules, rip-up clasts of peat, and/or pebbles. Fluid-escape structures and frost cracks (Murton et al., 2000) are common.

Overbank deposition of sand and silt onto vegetated stream banks preserves buried soils containing in situ root layers of willow shrubs and thin strata of sedge (Cyperaceae) peat. Drapes of silty sand vary from massive-structured beds up to decimeters in thickness to centimeter-thick beds of trough cross laminae. Erosional contacts are rare, and fluid-escape structures and frost cracks are common.

Dune foreset deposits are fine to medium-grained sand in medium- to large-scale sets of high-angle (30–35°) cross strata dominated by grainfall, slump, and grainflow stratification (Hunter, 1977). Cryoturbation features (Koster and Dijkmans, 1988) occur occasionally. Along former slip-face aprons, the foresets of precipitation ridges typically overlie sand-sheet deposits or deposits of sand-dominated loess.

Sand-sheet deposits (Dijkmans and Koster, 1988; McKenna-Neuman, 1993) are common in the GKSD, and all three of Lea's (1990) sand-sheet facies are present. One end member consists of wedge-like sets of thin, inversely graded laminae of fine to medium sand containing rare ripple foresets (Lea, 1990). Lags of coarse sand grains or isolated, convex-upward lenses of coarse sand mark truncation surfaces (McKenna-Neuman and Gilbert, 1986). Organic material and root

mottling are rare. The other end member contains undulatory, alternating, subhorizontal strata of fine to medium sand, whose internal structure ranges from massive to well-laminated. Coarse-grained wind ripples and deflation lags are rare. Bedding packages and internal strata pinch and swell and terminate along strike. Depositional contacts are wavy and irregular (Kolstrup and Jorgensen 1982). Some strata are faintly oxidized, and root mottling and in situ root systems are locally abundant. Today, sand sheets occur near the margins of the GKSD, notably along the eastern side of the dunes and at the edges of vegetated patches within the dunes (Dijkmans and Koster, 1990).

Sand-dominated loess deposits form a distinct and widespread sedimentary facies near the GKSD. Sand that is transported out of the dune field rains on vegetated surfaces, where it covers and eventually becomes interstratified with soil organic horizons. Deposits of sand-dominated loess differ from sand-sheet deposits by containing a greater amount of interstratified organic material and by lacking evidence for aeolian-traction processes. The internal structure of the sandy strata is massive. Sand strata range from laminae to beds several centimeters thick, and they pinch, swell, and terminate along strike. Contacts between beds are wavy and irregular and often disrupted by root channels. Sporadic zones of oxidation and traces of soil O- and E-horizon development record incipient soil formation. Post-depositional deformation of sandy strata is common, probably caused by cryoturbation (van Vliet-Lanoë et al., 1993) and by the decay of organic material. The organic matter in sand-dominated loess deposits includes humus, charcoal, terrestrial snails, mammal bones and woody material, including logs. Today, most deposition of sand-dominated loess occurs where precipitation ridges are invading forests.

Soil development around the GKSD is dominated by podzolization accompanied by the accumulation of thick organic horizons. These organic horizons contain abundant charcoal derived from the area's frequent wild fires. When buried under unweathered sand near the former slip-face apron of a precipitation ridge, podzolic profiles provide a convenient marker for a preceding interval of surface stability.

5. Results and discussion

5.1. Stratigraphic sections

5.1.1. Kavet creek

Flowing northward along the lower slopes of the Waring Mountains, Kavet Creek is forced by topography to trace closely the western margin of the dune field. Its cutbanks expose several stratigraphic sections of interest for dune-field history. Section AR (Fig. 4) is a 150 m long cutbank that exposes floodplain and sand-sheet deposits at creek level overlain by 2–8 m of fluvial sands. These fluvial sands evidence several episodes of stream aggradation. In the upstream part of the cutbank, subsection A, trough cross-laminated sands bury a rooted willow dating to $>40{,}000$ ^{14}C yr BP (Fig. 5) (Appendix A, Table 1(a)). A more recent aggradation interval dates to around 1400 ^{14}C yr BP, the age of a 25 cm diameter spruce log interbedded with trough cross-laminated sands containing pebbles and cut-and-fill structures in subsection Z. The calibrated age of a twig dated to 1530 ± 50 ^{14}C yr BP, from fluvial sands underlying aeolian sand-sheet deposits in subsection A suggests this episode of stream aggradation

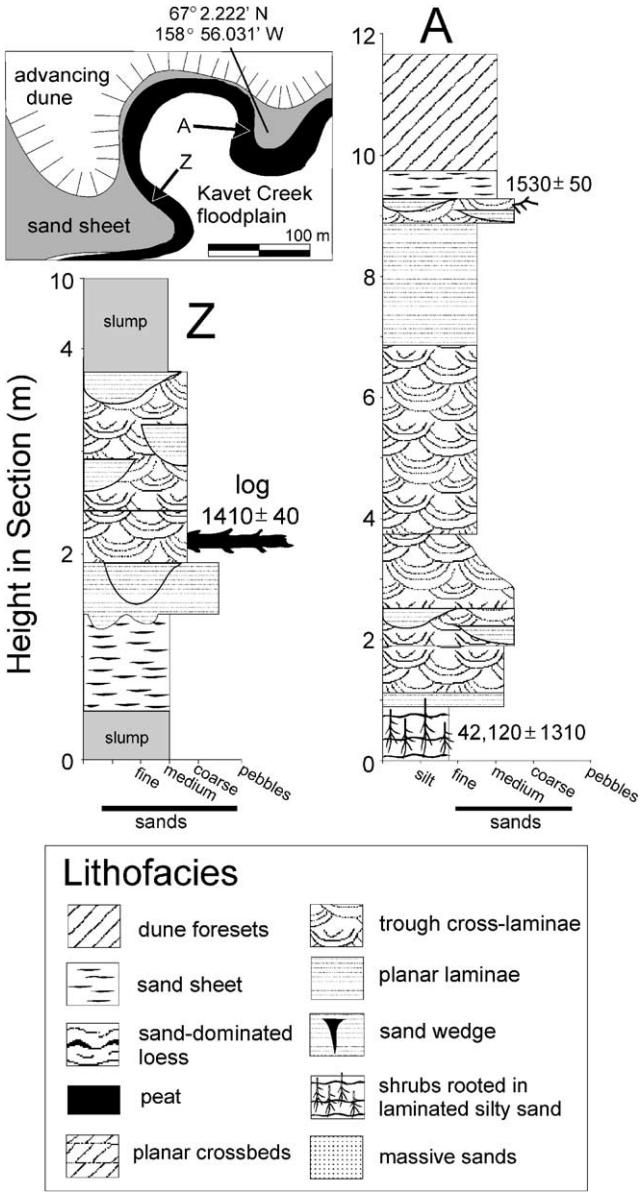

Fig. 4. Section AR along upper Kavet Creek.

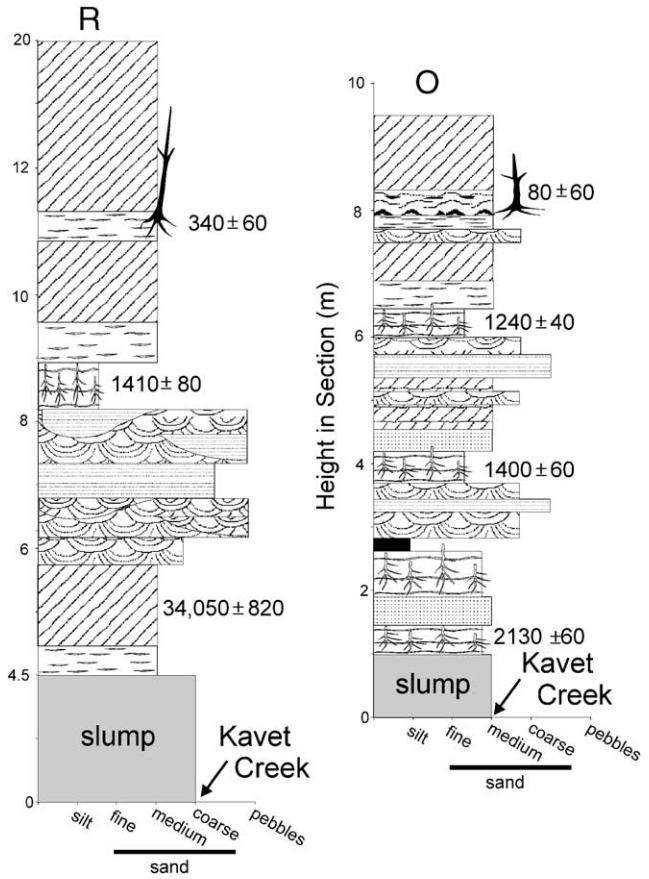

Fig. 5. R and Oasis–Amphitheater sections along Kavet Creek. See Fig. 4 for key.

ended ~9 m above the present stream level at 1180–1410 cal yr BP. The foreset beds left by an advancing dune slipface overlie the sand-sheet deposits (Fig. 4). Numerous, unpaired stream terraces occur along the western side of Kavet Creek near this section and indicate that the creek has recently been downcutting. A vegetation cover of willow and young white spruce, together with poorly developed soils with thin organic horizons suggest these terraces have an age range of 10–100 yr.

Six kilometers downstream from the section just described, Kavet Creek intersects a high dune slipface at Section R (Fig. 5). The lower 6 m of the section contain sand-sheet deposits overlain by dune foresets. Graminoid stems in foreset strata date to 34,000 ^{14}C yr BP (Table 1(b)). Several meters of fluvial deposits, including channel-fill gravels, overlie these Pleistocene dune sands and in turn are overlain by floodplain sediments. Willow shrubs rooted in the floodplain deposits date to 1410 ^{14}C yr BP (Table 1(a)), and they indicate that the floodplain of Kavet Creek was ~9 m higher at that time, consistent with subsection Z described above. Thick, dune-foreset deposits containing occasional sand-sheet units complete the section and indicate that dunes buried the former floodplain sometime after 1400 ^{14}C yr BP. A lone spruce tree that died sometime during the last 500 yr (Table 1(c)) is rooted in sand-sheet deposits 11 m above creek level (Fig. 5). Today, fluvial erosion exceeds aeolian deposition at this site, and the creek is eroding laterally into dune sediments. Abundant unpaired terraces covered with youthful vegetation and soils suggest recent, rapid downcutting in this reach of Kavet Creek.

A complex sequence of aeolian and fluvial sediments is exposed in "Oasis Amphitheater" near the northwestern end of the GKSD (Fig. 3). At creek level, peaty floodplain deposits containing rooted willow shrubs date to 2130 ^{14}C yr BP (Fig. 5, section O) (Table 1(b)). Above, 4 m of alternating fluvial sands and organic floodplain deposits indicate that floodplain aggradation occurred between 2100 and 1240 ^{14}C yr BP. Sand-sheet deposits directly overlie floodplain deposits dated to 1240 ^{14}C yr BP and in turn are buried by dune foresets. Thin strata of trough cross-beds within the aeolian units indicate that the stream was continuing to aggrade as the dunes expanded westward across the Kavet Creek valley. Today a low dune is moving westward across the top of the section and burying a sand-sheet deposit containing rooted, dead spruce trees. Kavet Creek is eroding laterally into the dune sediments today. As is the case upstream, abundant unpaired terraces with youthful vegetation and soils suggest recent, rapid downcutting.

5.1.2. Ahnewetut creek

Ahnewetut Creek crosses the GKSD and exposes sections through inactive precipitation ridges of two different ages where it exits the dunes (Fig. 3). We exposed sections A1 and A2 by digging into the flank of a precipitation ridge whose crest is 16 m above creek level. This ridge (IV) demarcates the northeastern margin of a formerly more extensive GKSD (Fig. 6). Section A1 exposes the boundary between the foreset beds of the advancing precipitation ridge and underlying sand-sheet deposits (Fig. 7). The fragile shells of six terrestrial snails from a centimeter-thick lens of organic debris within the dune foreset strata date to 3730 ^{14}C yr BP (Table 1(a)). The lower 2.2 m of section A1 are deposits of sand-dominated loess underlain by fluvial sands. These fluvial sands were deposited when Ahnewetut Creek had aggraded ~8 m higher than its present level. We interpret section A1 as recording the approach of a precipitation ridge coincident with increasing bedload in the creek and an aggrading floodplain. The precipitation ridge overran the site shortly after 3730 ^{14}C yr BP.

Section A2 lies 30 m beyond the outer slope of the same precipitation ridge exposed in A1 (Fig. 7). Here several meters of sand-dominated loess and sand- sheet deposits overlie fluvial sands deposited as high as 7.5 m above present creek level. Charcoal and spruce-cone fragments from the base of the sand-dominated loess deposit date to 3010 ^{14}C yr BP, indicating that a change from a sparsely vegetated sand sheet to a forest occurred

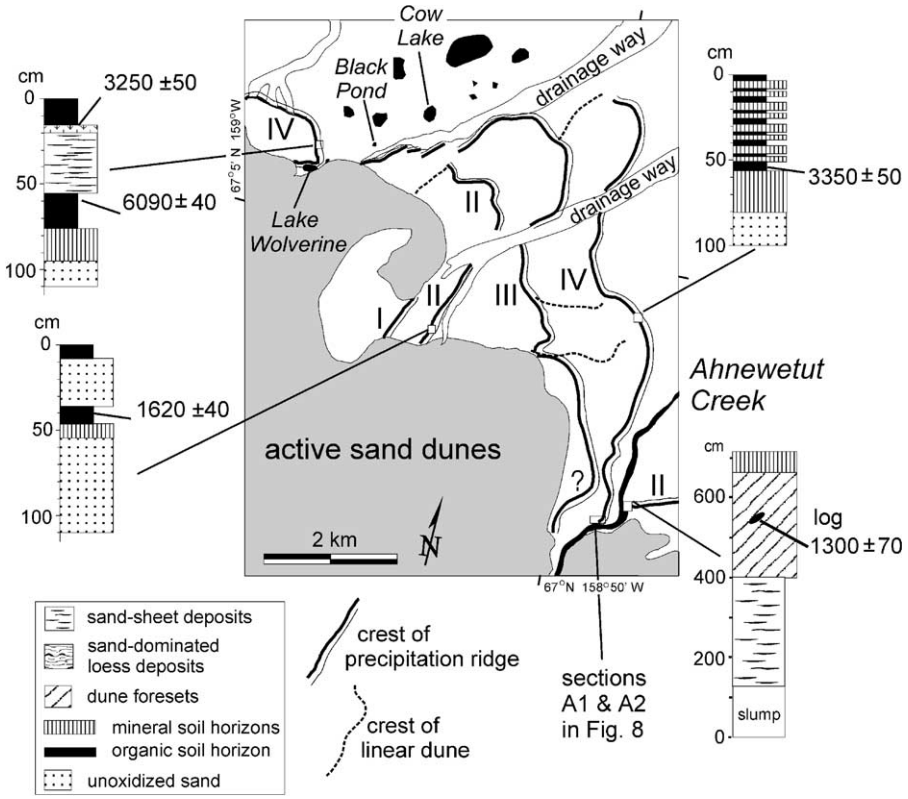

Fig. 6. Location of precipitation ridges along the northeast side of the GKSD together with stratigraphic sections used to date these ridges.

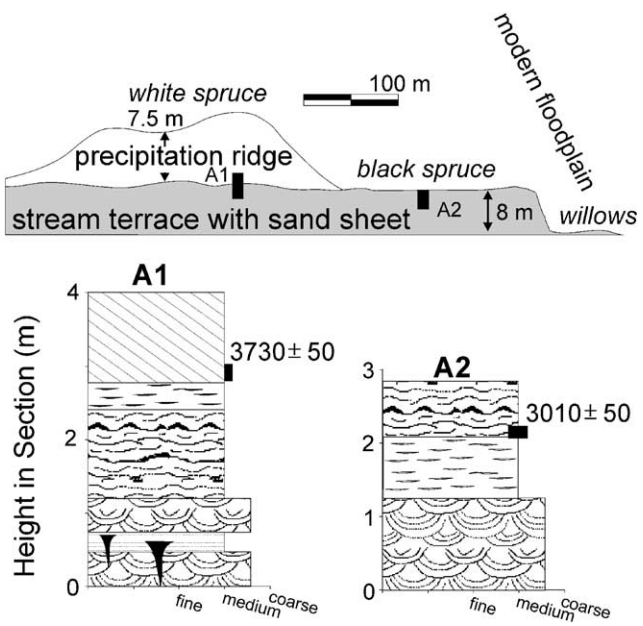

Fig. 7. Sections along Ahnewetut Creek where it exits the GKSD. At top is a schematic cross-section through stabilized precipitation Ridge IV. See Fig. 4 for key.

before that time. This implies that the nearby precipitation ridge stabilized before 3010 ^{14}C yr BP. Together, the Ahnewetut sections suggest that precipitation ridge IV (Fig. 6) stabilized between 3700 and 3000 ^{14}C yr BP. Also they record a period of aggradation in the Ahnewetut valley that preceded stabilization of Ridge IV and that probably was coincident with dune-field expansion.

On the south side of Ahnewetut Creek, a cutbank exposes a section through another precipitation ridge, which probably is coeval with Ridge II west of the creek (Fig. 6). Here several meters of sand-sheet deposits were buried by dune foresets. A compressed log from these foresets dated to 1300 ^{14}C yr BP and indicates stabilization of the precipitation ridge after that time (Table 1(c)).

5.1.3. Stabilized precipitation ridges

Episodes of dune-field expansion during the middle and late Holocene left four precipitation ridges in the forest northeast of the GKSD (Fig. 6). These ridges are up to 10 km long, and they stand 4–8 m above the land surface. After describing numerous soil profiles on vegetated dune crests, it became apparent that repeated episodes of soil erosion following fires made it impossible to use the degree of soil development for correlations. Instead, we correlate these ridges across drainages on the basis of their associated tree-ring and ^{14}C ages (Table 1(c)).

Cores taken with an increment borer from four white spruce trees growing on Ridge I revealed pith dates between AD 1910 and 1940. Wood fragments in the

organic horizon of a soil buried by inorganic sand along the distal slope of Ridge II dated to 1620 ^{14}C yr BP (Fig. 6). Ridge stabilization occurred some time after that time. A precipitation ridge south of Ahnewetut Creek is probably coeval with Ridge II north of the creek. As described above, a log dating to 1300 ^{14}C yr BP is embedded in dune foresets. Ridge II probably stabilized within several centuries after this time. We failed to find soils containing datable material along the distal margin of Ridge III.

Ridge IV is the outermost, morphologically intact precipitation ridge, and it extends more than 4 km from the active dune field. On the crest of Ridge IV near Ahnewetut Creek, the lowest charcoal in a buried soil organic horizon dates to 3350 ^{14}C yr BP, indicating ridge stabilization before that time. A similar, upper-limiting age comes from a soil pit at the base of the distal slope of a large precipitation ridge near Lake Wolverine (Fig. 6). Here a soil containing charcoal dating to 6090 ^{14}C yr BP was buried by sand. In the same pit, the modern organic horizon contained charcoal near its base dating to 3250 ^{14}C yr BP. On the basis of these limiting ages, Ridge IV formed sometime between 6100 and 3200 ^{14}C yr BP.

5.2. Ages of buried forests and soils

Wind erosion within the active dunes exposes paleosols buried by sand. Podzolic paleosols of several different ages are widespread in the northwestern and western parts of the GKSD. The best-developed profiles have E horizons 5–15 cm thick and Bw horizons up to 50 cm thick. The organic horizons of these paleosols contain charcoal, wood fragments, spruce needles, cones, and mammal bones, notably the mandibles of small mammals. ^{14}C ages from the paleosols range from 7000 to 1300 ^{14}C yr BP (Table 1(d)), though most cluster between 2200 and 1300 ^{14}C yr BP. For these soils to develop at a site, dunes had to be stabilized there.

In contrast, the ages of woody debris buried by sand but not associated with well-developed paleosols record episodes of dune-field activity (Table 1(e)). Interdune swales commonly contain conifer trees in growth position that are buried by aeolian sand (Fig. 8). Today, trees are being buried and killed by dunes both along the dune-field margin and in vegetated, interdune swales. In both these settings, soil development is only in its incipient stages. We interpret the ages of trees and organic debris associated with immature soils as close maximum-limiting ages on times of dune movement. Although blowing sand continually buries trees in the GKSD, changes in the frequency of buried-tree ages indicate changes in the overall activity of the dune field (c.f., Filion, 1984; Wolfe et al., 2000). ^{14}C ages from the GKSD indicate two peaks in tree-burial during the last 1500 yr, one centered on 1100 ^{14}C yr BP and another following 500 ^{14}C yr BP (Table 1(e)). We found only a few older samples; one suggests dune activity 3400–3000, another 7200–6800 ^{14}C yr BP.

Fig. 8. Spruce trunks exhumed by wind erosion in interdune swale at GKSD. Trunks lean westward in the migration direction of the precipitation ridge that buried them. Outermost wood from tree where coat is hanging dates to 250 ± 50 (Beta-109737).

6. Part II: lake cores

6.1. Study lakes

We cored two dune-marginal lakes to retrieve records of sand influx. "Lake Wolverine" is a cold, clear, freshwater lake approximately 500 m in diameter with a depth of 4 m in its flat, central basin (Figs. 3, 9). It has no inlet or outlet streams, and the lowest point of potential overflow is 4–6 m above the lake's surface. Discharge and recharge occur by groundwater flowing through the sands forming the basin. By analogy with similar lakes elsewhere (Almendinger, 1990), we expect the level of Lake Wolverine to be sensitive to changes in effective moisture. The landscape north of the lake slopes down to the Kobuk River and is covered by forested and highly eroded dune forms. There is little potential for more recently active dunes altering water level in Lake Wolverine by blocking downslope drainage (cf., Loope et al., 1995). The active slipface of an 8 m high dune forms the southeastern shore of Lake Wolverine. The lake is bordered on its other sides by stabilized precipitation ridges and blowouts, which are now densely vegetated. There is no evidence for mineral sediment entering the lake except along the dune slipface and by sand blowing across the ice in winter. In April 1998, snowdrifts several meters thick extended 10–20 m onto the lake ice in the lee of the adjacent dune slip face. The lake ice contained abundant sand near the active dunes. Along its vegetated margins, the lake is ringed by low sand berms covered by willow shrubs and sedges. These berms suggest that the summer water level of

Fig. 9. Lake Wolverine in early September 1998. Dune slipface enters lake in foreground. Coring raft in lake center. Active dunes visible in background. Note dense vegetation around other sides of lake.

Lake Wolverine has been as much as 1.5 m higher sometime during the past several decades. When we visited the pond in the summers of 1995, 1997, and 1998, water level was consistently below the lowest vegetated berm. Aquatic vegetation includes sparse stands of *Ceratophyllum demersum* and several *Potamogeton* species. Beaver activity was not observed in the watershed.

"Thigh-Deep Pond" (67° 5.244′ N, 159° 1.314′ W) lies in the forest 500 m west of the active sand dunes bordering Kavet Creek (Fig. 3). The pond is 15 m in diameter, and water depth reaches 2 m. It is located in a depression between stabilized dunes, and it overflows towards Kavet Creek through a swampy seepage zone. Aquatic mosses cover the pond's bottom, and *Carex aquatilis* grows around the shoreline. White spruce, black spruce, and willow shrubs surround the pond. Sand is abundant in moss polsters on tree branches near Thigh-Deep Pond, indicating that aeolian sand is arriving there from the dunes. No beaver activity was observed in the watershed. We cored "Cow Lake" and "Black Pond" to obtain basal ages on organic sedimentation in order to estimate the timing of dune-field stabilization. Both are located in forested basins within dune topography.

7. Methods

We cored Lake Wolverine, "Black Pond", and "Cow Lake" in mid-April 1997, using a modified Livingston corer (Wright et al., 1984) through lake ice. In September 1998, we took additional sediment cores from Lake Wolverine and a core from Thigh-Deep Pond using a pistonless, percussion corer operated from rafts. Altogether, we took ten sediment cores from Lake Wolverine in two clusters 5 m in diameter and spaced 25 m apart in the lake center. We studied multiple cores in order to obtain sufficient plant macrofossils for radiocarbon dating and to control for within-lake variability in sedimentation.

Cores were split in the laboratory and sampled at 0.5 cm intervals (September Core 1) and 1 cm intervals (April Core 1). The outermost sediments were removed to prevent contamination between adjacent stratigraphic levels. Stratigraphy was described by examining smear slides of sediment at 1 cm intervals. Particle size (Udden–Wentworth scale) of mineral sediment was determined by dry sieving following the removal of organic material and carbonate using HCl and H_2O_2. Mass accumulation rates (MARs) were calculated by multiplying mass per unit volume ($g\,cm^{-3}$) by sedimentation rate ($cm\,yr^{-1}$). Magnetic susceptibility was measured on subsamples using a Bartington MS-2 susceptibility meter. Organic-matter content was estimated after loss on ignition at 500°C. Total inorganic carbon content was measured by subsequent heating of the same samples to 1000°C (Dean, 1974). We estimated the weight percentage of $CaCO_3$ by dividing weight losses between 500°C and 1000°C by a factor of 0.44 (Hu et al., 1996). Mineralogy was determined by standard X-ray diffraction techniques (Chen, 1977).

Dating control in lake-sediment cores came mainly from the accelerator mass spectrometry (AMS) radiocarbon ages of plant macrofossils. We extracted plant macrofossils from core subsamples by washing sediment through 250 μm sieves and examining residues under a dissecting microscope. We determined recent sedimentation rates by the position of the ^{137}Cs peak and profiles of ^{210}Pb (Krishnaswami and Lai, 1978).

To reconstruct the history of sand accumulation in Lake Wolverine, we combined the AMS ages from all 10

cores after correlating these cores using multiple stratigraphic markers. The most important of these markers were marl layers of varying thickness and spacing that provide a detailed, stratigraphic "bar code" within Lake Wolverine. We calculated regression equations relating the depths of specific marl layers in one core with their depths in other cores. These regression equations, which all had r^2 values >0.99, were used to determine the stratigraphic positions of ^{14}C ages in two master cores (September Core 1 and April Core 1). These placements were confirmed, and in some cases refined, by magnetic susceptibility logs, by comparisons of organic-carbon content, and by the locations of sediment-type boundaries (Fig. 10).

Age–depth curves were plotted as error envelopes derived from the 2-sigma errors of the ^{14}C ages combined with the core interval from which each dated macrofossil was taken. An error of ± 1 cm was assumed in all depth measurements. Error envelopes were outlined by the corners of the boxes formed by plotting the least possible depth of each AMS sample against the greatest possible calibrated sample age and vice versa. After calibrating ^{14}C ages (Stuiver et al., 1998), we calculated a series of spline equations describing the two depth-age curves outlining the maximum error envelopes of September Core 1 and April Core 1. These splines were calculated as linear or polynomial regressions and spline length (number of dated intervals included) was constrained to keep r^2 values $\geqslant 0.99$. Though tedious, this procedure avoided the inaccurracies involved in using a single polynomial equation to describe an age–depth relationship in a setting where sedimentation rate is inconstant (Bennett, 1994). These age–depth relationships were used to calculate time series of mineral accumulation. The age–error envelopes in plots of mineral accumulation rates are based on the errors associated with age–depth relationships.

8. Results and discussion

8.1. Lake wolverine

8.1.1. Stratigraphy and sediments

Above inorganic basal sand, sediments in Lake Wolverine alternate between peat, marl, and algal mud, all of which contain abundant sand. Depths and thicknesses vary between the September and April cores due to differences in compaction caused by the different corers. We use the longest cores to illustrate the general stratigraphy.

The April core series penetrated to inorganic, medium sand 240 cm below the water/sediment interface (Fig. 10). At a depth of 234 cm, a layer of sandy graminoid and moss peat overlies this inorganic sand along an abrupt boundary. At the 225 cm level, sandy algal mud (gyttja) first appears and is interlayered with aquatic moss (cf. *Scorpidium*). At the 218 cm level, gyttja is abruptly replaced by a 40 cm thick unit of sandy chalk (Kelts and Hsũ, 1978). This chalk is yellowish gray in color and has a wavey, laminated structure. X-ray diffraction of three chalk samples revealed low-Mg calcite and quartz. Calcium carbonate comprises up to 90% of the chalk unit by weight. Aquatic mosses are interlayered with the chalk within several centimeters of its upper boundary. A layer of graminoid and moss peat containing vole feces and woody rootlets overlies the chalk unit between depths of 177 and 163 cm (Fig. 10). From a depth of 163 cm upwards, sediments consist of interstratified, sandy marl and sandy gyttja. X-ray diffraction at two levels revealed the marl to contain low-Mg calcite.

In the September cores, medium, fine, and very fine sands were the predominant particle sizes of non-carbonate mineral material in 102 sieved samples (Fig. 11). Very coarse sand and silt were always $<20\%$ and usually $<5\%$. Throughout Lake Wolverine's sediments, organic-matter percentages range from 5% to around 50% (Fig. 12). Magnetic susceptibility is correlated with non-carbonate, mineral concentration ($magnetic\ \ susceptibility = 0.02 \times + 0.03, \quad r^2 = 0.60$). Above the chalk layer, $CaCO_3$ occurs as laminae and diffuse beds within the gyttja, and locally it comprises 20–30% of sediment mass.

8.1.2. Depth-age models

We constructed separate depth–age models for the September and April core series as the first step in calculating MARs. The two models share most of their dating control (Fig. 13) (Appendix B). Only one age, Beta-123321 from September Core 1, could not be securely correlated into April Core 1. Three ages plotted slightly outside the error envelopes of both cores and were not used in either age model (Fig. 13). These samples (Beta-123320, Beta-125085, and Beta-123326) consisted of a charred twig, an uncharred twig, and a wood fragment, respectively. All three samples showed evidence of surface wear including the removal of bark and the rounding of broken edges. The dated samples used in the age models were non-woody macrofossils, mostly spruce needles and seeds. Reworked charcoal and wood fragments commonly occur in the active dune field downwind of interdune swales where buried forest layers are being exhumed by wind erosion. We suspect that the three, slightly age-discordant samples were blown into Lake Wolverine from buried forests located upwind.

Potential errors in estimating the age/depth curves from Lake Wolverine yield an overall temporal resolution for the records of ± 150–200 yr. The mean age error in April Core 1 is 178 yr (SD = 72) with a minimum of 13 yr near the core top and a maximum of 490 yr around

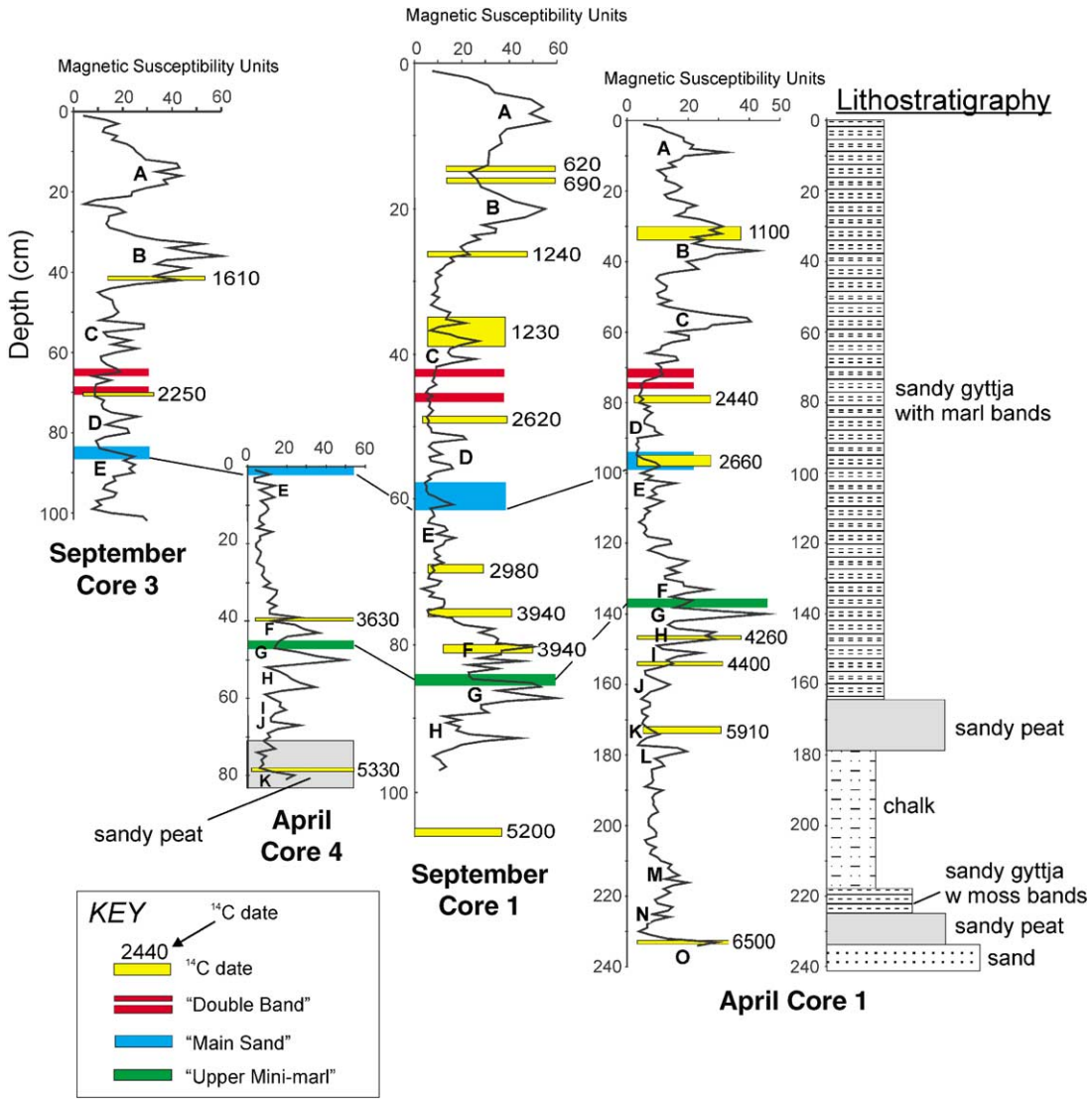

Fig. 10. Stratigraphic correlations between four sediment cores from Lake Wolverine. Space does not allow all 10 cores to be shown. ^{14}C dates, together with the depth interval from which the sample came, are shown as yellow boxes. Refer to Appendix B for complete information on these dates. Prominent peaks in magnetic susceptibility are labeled with letters. Lithostratigraphy of April core 1 at right side.

the level of 6500 cal yr BP. The mean age error in the September core is 156 yr (SD = 91) and ranges from a minimum of several years near the core top to 410 yr at core base.

8.1.3. Mass accumulation rates

The MARs of non-carbonate mineral material and carbonate into Lake Wolverine fluctuated markedly over the last 7500 yr (Fig. 14). Where the core series overlap, they record similar patterns of non-carbonate mineral MARs with four periods of rapid accumulation during the last 5000 yr (Fig. 14). The pattern of carbonate MARs also are similar between the two core series and generally correspond to peaks in sand MARs. High MARs of carbonate occurred 7400–6800, 5000–4000, 1300–600, and within the last several hundred cal yr BP (Fig. 14).

Sieving of the upper portion of the September cores and smear-slide examination of both cores indicate that the non-carbonate mineral material is mostly very fine to medium sand. Changes in the MAR of sand into lake Wolverine were accompanied by changes in particle size, with deposition of coarser sands accompanying high sand MARs (Fig. 15). For instance, when the MAR of sand was high for several centuries before and after 1000 cal yr BP (Fig. 14), abundant medium sand was deposited episodically. During periods of low sand MAR, for instance between 2000 and 2500 cal yr BP, very fine sand was more abundant.

8.2. Thigh-Deep Pond

The history of sand input into this shallow pond is similar to that observed in Lake Wolverine over the last

1000 yr (Fig. 16). Compact sediments prevented coring deeper than 90 cm below the water–sediment interface in Thigh-Deep Pond. Its sediments consist of laminae of aquatic moss separated by beds and laminae of fine and very fine sand and sandy gyttja. Magnetic susceptibility is a proxy for non-carbonate mineral concentration, and susceptibility measurements indicate a peak in sand concentration at levels dating to 600–800 cal yr BP. Sand input was low until after 470 cal yr BP, then increased to a minor peak between that time and the present. We correlate the two intervals of increased sand input into Thigh-Deep Pond with Episodes I and II of high sand MAR into Lake Wolverine (Fig. 16).

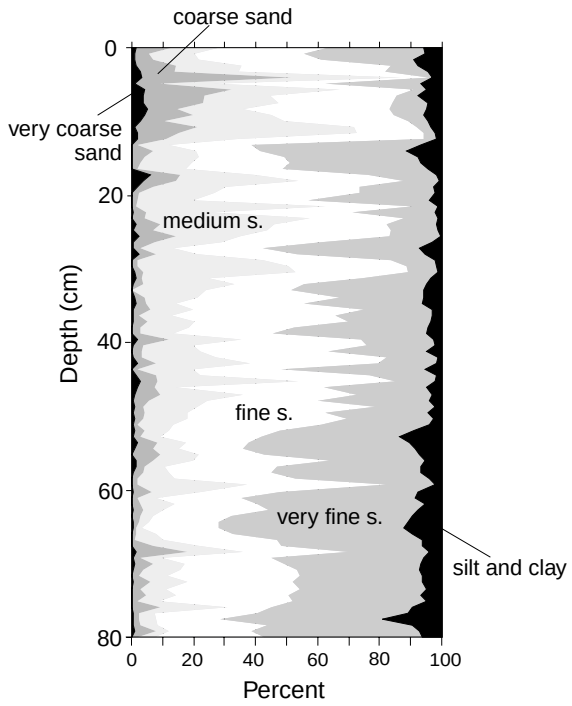

Fig. 11. Particle size as stacked weight percentage in September core 1.

9. Part III: synthesis

9.1. Lake Wolverine and dune-field history

Are the mass accumulation records of sand and carbonate from Lake Wolverine proxies for events in the entire GKSD? Field observations indicate that the amount of sand entering the lake today depends on the proximity and activity of the dune field. The record of sand concentration from Thigh-Deep Pond resembles that from Lake Wolverine, suggesting a common history of sand input from the dunes over the last ca. 1000 yr despite their locations on different sides of the dune field. Stratigraphic sections elsewhere in the GKSD also agree with the Lake Wolverine MAR record, indicating that the Lake Wolverine cores provide a valid proxy for changes in the extent and activity of the entire dune field.

The record of dune-killed vegetation extends back to around 1500 ^{14}C yr BP and mirrors the Lake Wolverine record. We assume that the ages of erect tree trunks buried by aeolian sand and the ages of plant debris in poorly developed paleosols (Table 1(e)) provide close, maximum-limiting ages on periods of dune-field expansion. Their ages cluster around the times of Episodes I and II in Lake Wolverine (Fig. 17). The ages of wood and charcoal samples associated with well-developed, buried soils in the active dune field clump together in the 2200–1300 ^{14}C yr BP interval. During this interval, large portions of the western GKSD apparently were stabilized under spruce forest, and this was a period of low sand influx into Lake Wolverine (Fig. 17). Limiting ages

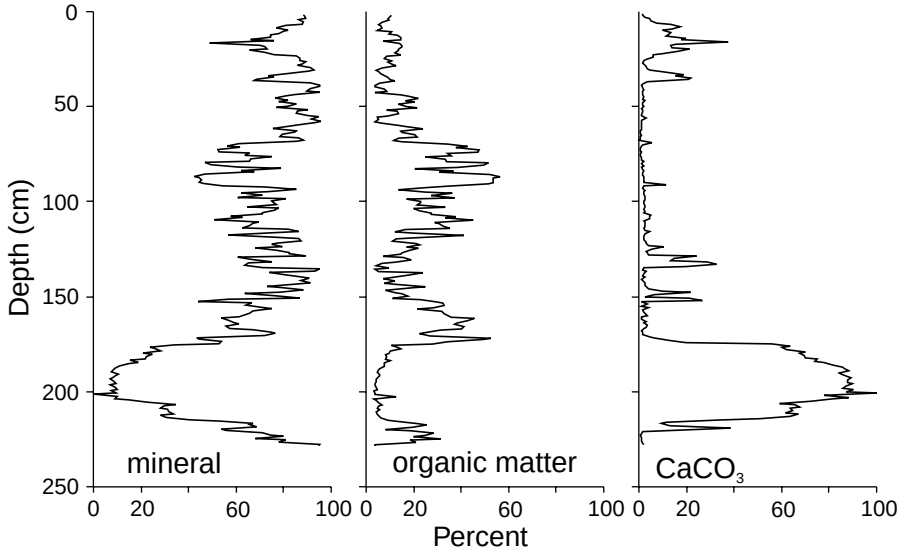

Fig. 12. Weight percentages of non-carbonate mineral material, $CaCO_3$, and organic matter in April core 1.

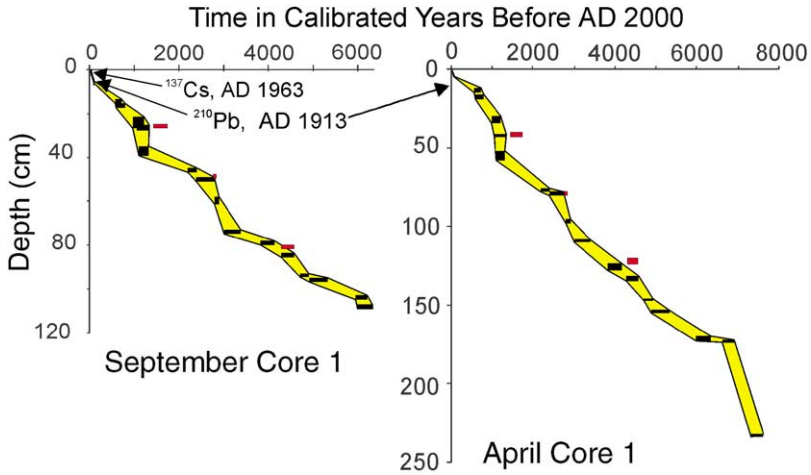

Fig. 13. Depth/age curves in Lake Wolverine cores. Boxes show error estimates of individual dates. Red boxes are ^{14}C dates on wood fragments not used in curve construction.

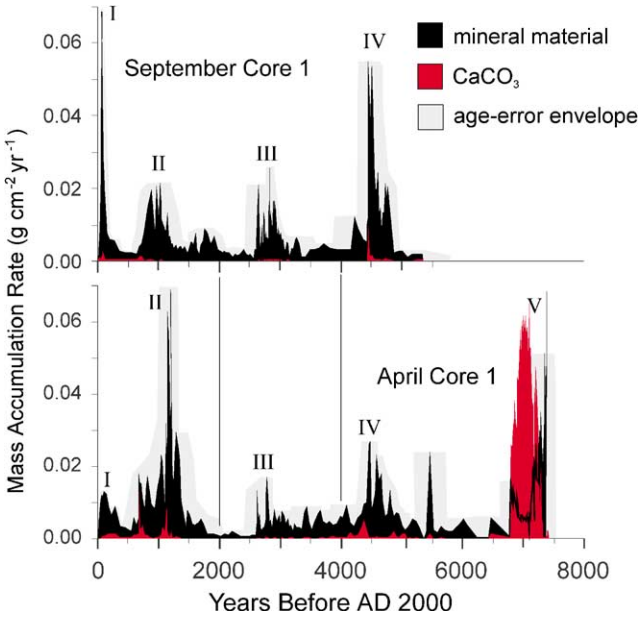

Fig. 14. Fluctuations in the influx of sand and $CaCO_3$ into Lake Wolverine. Episodes of high sand MAR are numbered I through V.

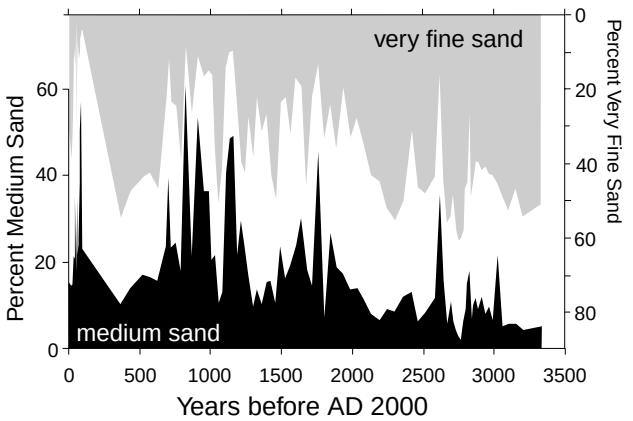

Fig. 15. Changes in the particle size of sand deposited in Lake Wolverine over the last 3000 years.

on precipitation ridges (Table 1(e)) suggest that several episodes of ridge stabilization took place. One occurred after 1500 ^{14}C yr BP, an earlier one ca. 3900 ^{14}C yr BP, possibly another sometime between 6100 and 3200 ^{14}C BP, and one ca. 7000 ^{14}C yr BP. However, these limiting ages are few in number and do little to constrain the Lake Wolverine record.

Limiting ages on periods of stream alluviation further support the wider applicability of the Lake Wolverine record. Today, during a period of relative quiescence in the dune field, streams are downcutting in and around the GKSD. An expanded and more active dune field causes floodplain aggradation by diverting streams upslope and loading them with sediments. Ages from sections along Ahnewetut and Kavet Creeks indicate that stream floodplains were significantly higher than today around 4000 cal yr BP at the close of Episode IV, a time of major sand input into Lake Wolverine (Fig. 17). Another period of stream aggradation occurred ca. 3000 cal yr BP during Episode III in the Lake Wolverine record. The floodplain of Kavet Creek was near its present level 2400–1500 cal yr BP, which was a period of low sand input to Lake Wolverine. Floodplains had aggraded many meters above their present levels 1500–900 cal yr BP during Episode II.

10. Climatic controls over the Kobuk dunes

The extent and activity of the GKSD during the Holocene has been controlled mainly by changes in effective moisture. We base this conclusion on the importance of effective moisture in determining dune-field activity elsewhere in the world and on correlations between the activity of the GKSD and water levels in Lake Wolverine.

In most environments, dune-field activity is controlled by some combination of four interacting factors: windiness, sand supply, vegetation cover, and effective moisture (Cooke et al., 1993; Muhs and Maat, 1993; Lancaster, 1995). The importance of changes in overall windiness for the Holocene activity of the GKSD is hard to assess. Changes in wind directions and velocities caused by retreating continental ice sheets have been implicated in the Holocene demise of dune fields in Canada (David, 1981; Filion, 1987); however, climate modeling suggests that such ice-sheet effects are unlikely for northwestern Alaska during the Holocene (Edwards and Barker, 1994; Bartlein et al., 1998).

Effective moisture controls vegetation cover and sand availability in many aeolian settings (Lancaster, 1995; Muhs et al., 1996; Clark and Rendell, 1998; Kocurek and Lancaster, 1999), and decreased effective moisture is a widespread cause of dune reactivation (cf., Madole, 1994; Tchakerian, 1994; Muhs and Holliday, 1995; Bullard et al., 1997; Muhs et al., 1997; Kocurek, 1998; O'Connor and Thomas, 1999). Sand supply at the GKSD is entirely from underlying, older dune sands, and the availability of these sands for dune building is determined by the height of the water table and by vegetation cover (cf., van Vliet-Lanoë et al., 1993; Seppällä, 1995). Both these factors are related closely to effective moisture. Potential evapotranspiration exceeds actual evapotranspiration today in the Kobuk valley, and drought stress impacts tree growth at well-drained sites throughout interior Alaska (Barber et al., 2000). In the GKSD, where active layers extend deeply into sandy soils, drought stress is probably an important control over vegetation cover and hence sand supply.

Further evidence for the important role played by effective moisture in the GKSD comes from correlations between dune-field activity and water levels in Lake Wolverine. Sediment stratigraphy suggests that the initially dry basin underwent a fluctuating trend towards increasingly wetter conditions between 7500 and 5000 cal yr BP during the onset of regional Neoglaciation, which accompanied relatively moist conditions throughout Alaska and northwestern Canada (Calkin, 1988; Moser and MacDonald, 1990; Cwynar and Spear, 1991, 1995; Anderson and Brubaker, 1994; Hu

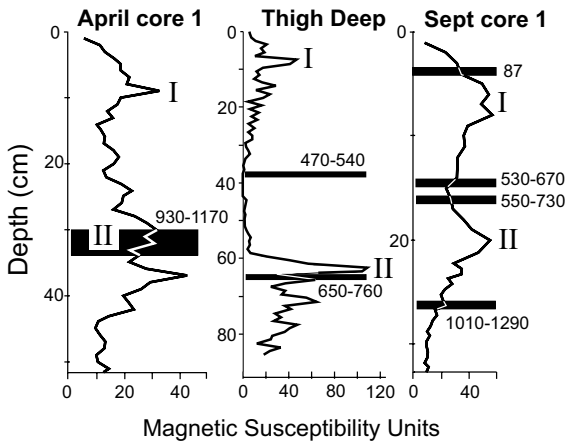

Fig. 16. Magnetic stratigraphy of Thigh-Deep Pond, center, compared with that of Lake Wolverine, right and left. High magnetic susceptibility readings signify high concentrations of mineral material. Black bars are uncalibrated ^{14}C dates with 2-sigma errors. See Appendix B for complete information on these dates. In right-hand graph, "87" is a ^{210}Pb date.

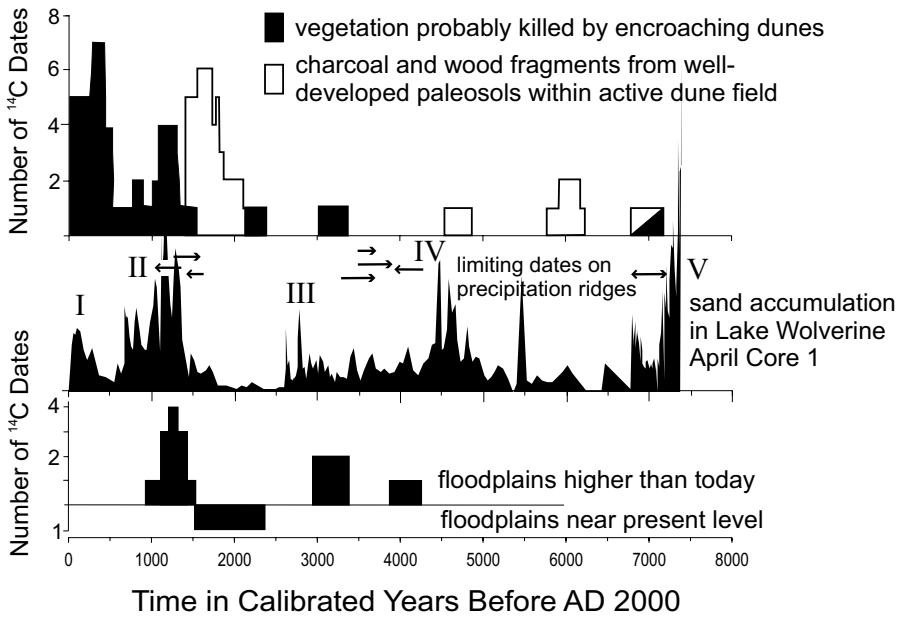

Fig. 17. Sand influx to Lake Wolverine compared to other indicators of dune-field extent and activity. ^{14}C ages shown as 2-sigma error widths. For histograms, the 2-sigma intervals of calibrated ^{14}C ages from Appendix A are sorted into decadal bins.

et al., 1998; Pienitz et al., 1999; Abbott et al., 2000; Anderson et al., 2000). The basin formed ca. 7500 cal yr BP as an interdune depression (Fig. 10). The new basin was briefly filled with sedges and mosses, which deposited peat. At this time, the Wolverine basin probably was moist throughout the year, but standing water did not occur during the growing season. The basin contained perennial, standing water after ca. 7400 cal yr BP, when algal muds were first deposited. Abundant deposition of calcium carbonate followed shortly afterward, suggesting that water level had fallen and the basin contained a perennial but shallow pond from ca. 7200–6700 cal yr BP. Sedge and moss peat again accumulated after ca. 6700 cal yr BP, indicating a return to drier conditions when the basin floor was moist but not submerged during the growing season. After ca. 5800 cal yr BP, water levels rose and the basin contained water throughout the year. Between 5800 cal yr BP and the present, carbonate and sand MARs in Lake Wolverine are positively correlated (Fig. 14), suggesting that the dune field was especially active when lake levels were low.

Carbonate precipitation in Lake Wolverine probably occurs through a combination of three processes, all of which are enhanced by dry climate. These processes include temperature's effects on solubility, evaporative concentration as the lake dries, and increased concentration of inflowing solutes when groundwater recharge declines. The partial pressure of CO_2 and hence the solubility of carbonate is lower in warm water than in cold. The upwelling of cold, carbonate-laden groundwater into the warm water of shallow lakes results in abundant $CaCO_3$ precipitation (Kelts and Hsũ, 1978). Dijkmans et al. (1986) identified temperature effects on solubility as the process causing calcrete formation in the GKSD. This process of carbonate precipitation may be especially important at high latitude sites where summer heating at the surface is intense, but the groundwater is very cold. When water level in Lake Wolverine drops, water temperatures become warmer in summer, and more carbonate precipitates. In addition, carbonate precipitation is enhanced by evaporative concentration when lake level falls. Finally, declining recharge upslope will slow the transit time of groundwater flowing towards Lake Wolverine. Longer transit times increase solute loading, which further augments the precipitation of carbonate in the lake basin.

The use of sedimentary $CaCO_3$ as a proxy for lake-level history could be complicated by changes in its preservation potential over time. In lakes in the American Midwest, levels of sedimentary organic matter $>25\%$ cause dissolution of $CaCO_3$ during sediment diagenesis (Dean, 1999). However, the antagonism between organic matter and sedimentary carbonate is not universal. Holocene-aged sediments of other arctic and subarctic lakes (e.g., Pienitz et al., 2000; Anderson et al., 2001) contain abundant carbonates despite organic matter percentages $>25\%$.

11. Inferences about paleoclimate

If our hypothesis about the importance of effective moisture in controlling dune-field activity in the Kobuk valley is correct, we can infer that July, August, and September are the critical months for climatic changes affecting moisture status in this area. In northwestern Alaska today, most of the annual precipitation occurs between July and October when the Bering and Chukchi Seas are ice-free, and North Pacific storms move northwards into the region (Moritz, 1979). The other determinant of moisture balance, evapotranspiration, is also concentrated during summer months. Although much of the sand movement at the GKSD occurs in the winter and spring, soil moisture throughout the year is controlled by precipitation and evapotranspiration during summer and early autumn. Significant fluctuations in climate during this seasonal window must have occurred over the last 8000 yr.

We can speculate about the shifts in atmospheric circulation that triggered changes in effective moisture at the GKSD. The simplest way to lower precipitation in northwestern Alaska is to exclude storms originating in the North Pacific. Mock et al. (1998) recognize a modern atmospheric circulation pattern in which the northeastern Pacific subtropical high is weakened in summer. Within this synoptic pattern, fewer Pacific storms reach northwestern Alaska, and precipitation decreases there. We suspect that periods of heightened aeolian activity in the Kobuk valley accompanied an increased incidence of this particular synoptic pattern.

Contrasting histories of dune fields in northern Alaska demonstrate a marked regionality of climate north and south of the Brooks Range during the mid- and late Holocene. A preliminary chronology of dune reactivation in the Ikpikpuk dune field on the North Slope of Alaska (Galloway and Carter, 1993) shows an antiphase relationship with the GKSD (Fig. 18). These contrasting histories may be due to the dune fields' locations relative to the Arctic Front (cf., Rabus and Echelmeyer, 1998), whose position in summer typically lies along the Brooks Range. High-latitude climate has varied markedly by geographic region over the last several decades (Maxwell, 1996; Briffa, 2000; Bradley, 2000), and strong differentiation of climate by region characterizes climate proxy data from arctic sites over the last several centuries (Overpeck et al., 1998).

No obvious correlations exist between the Kobuk dune record and glacier records from the Brooks Range, and we are not sure why. In a continental region like the central Brooks Range, equilibrium-line altitude is determined largely by summer temperature (Rabus

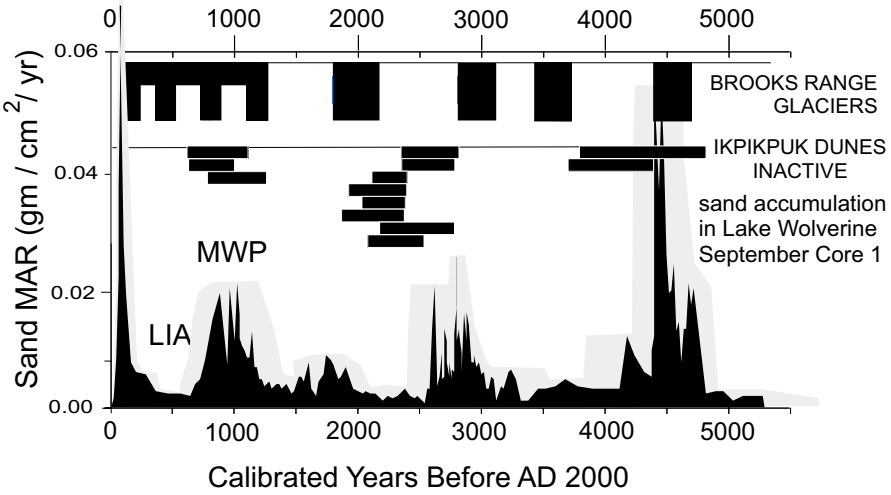

Fig. 18. Sand influx to Lake Wolverine compared to Holocene activity of Ikpikpik Dunes on the North Slope of Alaska (Galloway and Carter, 1993) and to glacier activity in the Brooks Range (Ellis and Calkin, 1984; Calkin, 1988). In glacial records, the black boxes are estimated times of glacier expansion.

and Echelmeyer, 1998). Warm summers in the Brooks Range should coincide with high pressure and low precipitation in at the GKSD, so glaciers should be retreating when the dune field is expanding. No obvious relation is discernible between the glacier and dune records. For instance, Ellis and Calkin (1984) noted glacier advances starting ca. AD 1200 and continuing through the Medieval Warm Period, which is evidenced as a major period of expansion at the GKSD.

12. Conclusions

By combining chronostratigraphic information from stream cuts, soil pits, dune-buried trees, and lake cores, we can reconstruct the history of the Great Kobuk Sand Dunes over the past 8000 yr. A period of dune-field stabilization occurred between 7000 and 5000 cal yr BP. After 5000 cal yr BP, four main episodes of dune-field expansion occurred at 400–1500 year intervals. The GKSD underwent marked expansion during the Medieval Warm Period, ca. AD 900–1400, was relatively inactive AD 1400–1800 early in the Little Ice Age (LIA), and expanded briefly late in the LIA prior to AD 1900. The dune field has shrunk over the last 80–100 yr. Moisture balance appears to be the major control of aeolian activity at the GKSD, as it is in other dune fields located in boreal-forest (Wolfe et al., 2000) and grassland ecosystems (Muhs and Maat, 1993). The history of dune-field extent and activity that we reconstruct is a proxy for regional moisture balance. The complex history of moisture balance changes in northwestern Alaska indicated by the GKSD record is probably related to shifts in the tracks of late-summer storms approaching the region from the North Pacific. Although temperature is usually regarded as the key variable mediating the impacts of climatic change on arctic and subarctic ecosystems, water balance may be the more proximal cause of environmental change in the Kobuk valley, and we suspect this is the case throughout the dry, interior regions of the boreal forest.

Acknowledgements

We thank Jeanne Schaaf, Peter Richter, Dale Taylor, Jess Grunblatt, and Lois Dollimolli of the United States National Park Service for their interest and support. Jeff Conaway and Fred Haering assisted in the field, and Andy Krumhardt in the laboratory. Carolyn Parker, David Marrett, Alan Batten, Ronald Sletten, and Mary Edwards made valuable contributions to our studies. We thank Tom Hamilton, Dan Muhs, Vance Holliday, and Margaret Smith for constructive reviews of earlier drafts of this article. Financial support came from the United States National Park Service's Shared Beringian Heritage Program. B.P.F. was supported by National Science Foundation grant ATM9707398.

Appendix A

Radiocarbon dates from the Great Kobuk Sand Dunes (see Table 1(a)–(f)).

Table 1

Sample	Laboratory number (Beta-)	Unofficial locality name	Location		Dated material	δ ^{13}C (‰)	^{13}C-adjusted radiocarbon age (yr before 1950 AD)[a]	2σ calibrated age range (cal yr before 1950 AD)[b]
			Lat (°N)	Long (°W)				
(a) *Dates relating to creek floodplains higher than today*								
9-12-96C	97352	Oasis Amphitheater, Kavet Creek	67°5′ 36.07″ 47.80″	159°0	Twig	−27.1	1240±60[a]	990–1290
9-15-96A	97354	R section, Kavet Creek	67° 4.455′ 59.679″	158°	Wood fragments	−26.9	1410±80[a]	1170–1510
7-31-98A	123314	AR section, Kavet Creek	67° 2.222′ N 56.031′ W	158°	Twig cf willow	−27.4	1530±50[a]	1180–1410
3Aug98oe	121019	Oasis Amphitheater, Kavet Creek	67° 5′ 36.07″ 0′ 47.80″	159°	Conifer in growth position	−27.5	1400±60	1180–1410
7-31-98aLOG	121016	AR section, Kavet Creek	67° 2.222′ 56.031′	158°	conifer log	−27.8	1410±40	1270–1390
PH97-22	111732	AR section, Kavet Creek	67° 2.222′ 56.031′	158°	Willow bush in growth position	−31.9	3010±60	3000–3360
9-7-97B	109754	A2 section, Ahnewetuk Creek	67° 2.8′ 49.4′	158°	Charcoal and *Picea* cone scale	−26.7	3010±50[a]	3000–3360
9-3-97XY[c]	109751	A1 section, Ahnewetuk Creek	67° 2.8′ 49.3′	158°	Terrestrial snails	−7.5	3730±50[a]	3930–4240
PH97-21	111731	AR section, Kavet Creek	67° 2.222′ 56.031′	158°	Plant fragments	−28.2	42,120±1310[a]	—
(b) *Dates relating to creek floodplains similar in altitude as today*								
3Aug98od	121018	Oasis Amphitheater, Kavet Creek	67° 5′ 36.07″ 47.80″	159° 0′	Twig in woody peat	−27.9	1790±60[a]	1550–1870
9-12-96A	97351	Oasis Amphitheater, Kavet Creek	67° 5′ 36.07″ 47.80″	159° 0′	Charred wood	−27.8	2130±60[a]	1950–2310
(c) *Limiting ages on formation of precipitation ridges*								
9-3-97A[c]	109740	Ahnewetuk Camp	67° 2.9′	158° 48.77′	Conifer log in dune foresets	26.2	1300±70	1060–1330
8-30-97E	109748	Niaktuvik Creek salient	67° 0.78′	158° 46.49′	Charcoal at base of modern O horizon	−26.2	1460±60[a]	1280–1520
9-18-98c[c]	125310	Precipitation Ridge II	67° 4.35′	158° 53.07′	Wood fragment in soil buried by precipitation ridge	−26.6	1620±40[a]	1410–1610
9-6-97C	109753	Lake Wolverine	67° 5.89′	158° 54.82′	Charcoal at base of modern O horizon	−24.6	3250±50[a]	3360–3630
8-29-97X	109744	LaBau	67° 4.52′	158° 48.42′	Charcoal in O horizon buried by episodic colluviation	−26.1	3350±50[a]	3470–3690
8-30-97D	109747	Niaktuvik Creek salient	67° 0.78′	158° 46.49′	Charcoal in buried O horizon	−26.8	3400±50[a]	3480–3830
9-3-97XY[c]	109751	A1 section, Ahnewetuk Creek	67° 2.8′	158° 49.3′	Terrestrial snails	−7.5	3730±50[a]	3930–4240
(d) *Wood and charcoal buried by sand and associated with well-developed podzolic soil profiles containing E and Bw horizons. Logs are lying on ground, stumps are root-crown portions of trees still in growth position*								
9-2-97B	111735	King Dune	67° 1.81′	158° 52.89′	Conifer log	−33.3	1680±60	1410–1710
9-2-97D	111736	King Dune	67° 1.81′	158° 52.89′	Conifer stump	−25.2	1680±70	1410–1730
9-11-96#2b	97350	Stump 2	67° 6′ 26.89′ 15.19″	159° 0′	conifer stump	−28.1	1700±80	1410–1820
9-18-98c[c]	125310	Precipitation Ridge II	67° 4.35′	158° 53.07′	Wood fragment in soil buried by precipitation ridge	−26.6	1620±40[a]	1410–1610

9-11-96A	97349	Nearest Camp	67° 6′ 23.32″ 40.83″	159° 0′	Conifer log	−27.9	1730±80	1420–1860
9-10-96F	97347	Rabbit	67° 6′ 19.67′ 48.07″	158° 59′	Charcoal and wood	−27.1	1800±50[a]	1570–1870
9-9-96B	97345	Barrel	67° 6′ 22.78″ 57.80″	158° 59′	Conifer log	−28.7	1930±90	1630–2110
9-10-96#2a	97348	Stump2a	67° 6′ 7.70″ 46.33″	159° 0′	Conifer log	−26.7	2080±60	1900–2300
9-9-96D	97346	Two Crowns	67° 6′ 7.07″ 44.42″	158° 59′	Outermost wood of conifer stump	−26.3	4210±50	4550–4860
9-2-97A	111734	King Dune	67° 1.81′	158° 52.89′	Charcoal in buried O horizon	−27.8	5190±60[a]	5750–6170
9-1-97A	109749	Harpoon Swale	67° 0.78′	158° 46.49′	Charcoal in buried O horizon	−26.2	5280±50[a]	5920–6200
9-6-97A[c]	109752	Lake Wolverine	67° 5.89′	158° 54.82′	Charcoal in buried O horizon (same profile as 9-6-96C)	−25.5	6090±40[a]	6800–7160
(e) *Wood or charcoal buried by aeolian sand but not associated with a well-developed soil. Tree trunks are standing erect and are buried by aeolian sand*								
9-12-96D	97353	Oasis Section, Kavet Creek	67° 5′ 36.07″ 47.80″	159° 0′	Outer wood, conifer trunk	−26.4	80±60	0–250
8-29-97A	109734	Cottonwood	67° 3.01′	158° 50.88′	Outer wood, conifer trunk	−25.0	150±50	0–300
9-1-97D	109738	King Dune	67° 0′ 9″	158° 50′ 34″	Outer wood, conifer trunk	−27.0	210±50	0–420
9-4-97A	109741	Exploded Moose	67° 2.2′	158° 55.58′	Outer wood, conifer trunk	−26.2	230±50	0–430
9-1-97C	109737	King Dune	67° 0′ 9″	158° 50′ 34″	Outer wood, conifer trunk	−25.9	250±50	0–460
8-1-98d	121022	R Section, Kavet Creek	67° 4.455′	158° 59.679″	Conifer tree in growth position	−27.0	340±60	290–510
8-29-97B	109735	Cottonwood	67° 3.01′	158° 50.88′	Outer wood, conifer trunk	−26.5	390±50	310–520
8-29-97C	109736	Cottonwood	67° 3.01′	158° 50.88′	Outer wood, conifer trunk	−26.2	510±50	500–630
9-6-97D	109743	East Side	67° 5.89′	158° 54.82′	Outer wood, conifer trunk	−26.6	810±50	660–880
8-30-97C	109746	Niaktuvik Creek Amphitheater	67° 0.27′	158° 47.98′	Conifer log in thin O horizon overlying dune foresets and buried by sand sheet	−28.5	960±50	740–960
9-1-97E	109739	King Dune	67° 0′ 9″	158° 50′ 34″	Outer wood, conifer trunk	−27.1	1130±50	930–1170
9-4-97B	109742	Exploded Moose	67° 2.19′	158° 55.53′	Outer wood, conifer trunk	−30.0	1210±50	990–1270
9-3-97A[c]	109740	Ahnewetuk Camp	67° 2.9′	158° 48.77′	Conifer log in dune foresets	−26.2	1300±70	1060–1330
9-1-97B	109750	Harpoon Swale	67° 1.52′	158° 54.56′	Outer wood, conifer stump	−28.0	1290±50	1070–1300
7-31-98a	123314	AR Section, Kavet Creek	67° 2.222′	158° 56.031′	Branch cf. willow overlain by sand sheet deposits	−27.4	1530±50[a]	1180–1410
8-30-97a	109745	Niaktuvik Creek Amphitheater	67° 0.27′	158° 47.98′	Conifer log in dune foresets	−27.5	2260±60	2120–2360
9-7-97B[c]	109754	A1 Section, Ahnewetuk Creek	67° 2.8′	158° 49.4′	Charcoal and Picea cone scale	−26.7	3010±50[a]	3000–3360
9-6-97A[c]	109752	Lake Wolverine	67° 5.89′	158° 54.82′	Charcoal in buried O horizon (same profile as 9-6-96C)	−25.5	6090±40[a]	6800–7160
(f) *Pre-Holocene radiocarbon ages*								
8-1-98a	121021	R Section, Kavet Creek	67° 4.455′	158° 59.679″	Graminoid stems	−29.0	34,050±820[a]	—
PH97-21	111731	AR Section, Kavet Creek	67° 2.222′	158° 56.031′	Plant fragments	−28.2	42,120±1310[a]	—

[a] AMS radiocarbon age.
[b] Using CALIB 4.0 of Stuiver et al., 1998.
[c] Sample ages pertaining to two categories.

Table 2

Sample	Beta analytic laboratory number-	Dated material	$\delta^{13}C$ (‰)	^{13}C-adjusted radiocarbon age (yr before 1950 AD)	2σ calibrated age range (cal yr before 1950 AD)[a]
Lake Wolverine					
SeptC1.15	123325	Twig with buds	−26.5	620±50	670–530
SeptC2.16-17	123324	Twig	−27.7	690±60	730–550
AprilC5e5	120590	4 spruce needles	−22.8	1100±50	1170–930
SeptC3. 41-42	123320	Charred twig	−25.1	1610±50	1690–1390
SeptC2.26-27	123323	Charred twig	−26.6	1240±50	1290–1010
SeptC1comb	127326	2 spruce seeds	−24.8	1230±40	1270–1060
SeptC3.70-71	127327	3 spruce needles	−28.2	2250±40	2350–2150
SeptC4.74-75	125085	Twig	−28.9	2620±40	2780–2710
AprilC2H2d1	118135	Leaves cf. willow with petioles	−25.8	2440±50	2730–2350
AprilC5MainSand		1 spruce needle, 1 leaf (*cf.* willow) midrib, bark fragment, wood fragment	−28	2660±40	2850–2740
SeptC2.69-70	123322	Wood fragment	−26.2	2980±50	3340–2970
AprilC4.39-40	127323	*Dryas* leaf, graminoid stem	−27.7	3630±40	4090–3780
SeptC2.75-76	123326	Wood fragment	−26.1	3940±50	4520–4240
SeptC2.80-81	123327	2 spruce needles	−28.9	3940±50	4520–4240
AprilC5 × 35	118134	2 spruce needles, twig	−28.5	4260±40	4870–4660
AprilC1.71	118136	Twig	−28.5	4400±50	5280–4850
SeptC2.95-97	123321	2 spruce seeds, 1 sedge seed, twig	−29.9	5200±40	6170–5910
AprilC4.78-79	127325	Rodent scat, woody rootlet	−27.8	5330±50	6280–5940
AprilC6basal twig 1	118131	Twig	−26.6	6500±60	7560–7270
AprilC5twig 5	119227	Twig	−28.7	5910±60	6870–6570
Thigh deep pond					
TD36-37	125084	Rodent (*cf.* lemming) scat	−25.1	460±40	540–470
TD64	125083	Bark fragment (*cf.* birch)	−26.1	770±40	760–650
Black pond					
BP+4-5	118132	8 sedge seeds, charcoal fragments	−28.4	7440±50	8370–8060
Cow lake					
CLbasal	118134	Graminoid stem	−30.3	12,270±50	15,440–13,850

[a] Using CALIB 4.0 of Stuiver et al. (1998).

Appendix B

AMS radiocarbon dates from lakes near Great Kobuk Sand Dunes (see Table 2).

References

Abbott, M.B., Finney, B.P., Edwards, M.E., Kelts, K.R., 2000. Lake-level reconstructions and paleohydrology of Birch Lake, Central Alaska, based on seismic reflection profiles and core transects. Quaternary Research 53, 154–166.

Almendinger, J.E., 1990. Groundwater control of closed-basin lake levels under steady-state conditions. Journal of Hydrology 112, 293–318.

Anderson, D.D., 1988a. Onion portage: the archaeology of a stratified site from the Kobuk River, northwest Alaska. Fairbanks, Alaska, Anthropological Papers of the University of Alaska 22 (1–2), 163.

Anderson, L., Abbott, M.B., Finney, B.P., 2001. Holocene paleoclimate from oxygen isotope ratios in lake sediments, central Brooks Range, Alaska. Quaternary Research 55, 313–321.

Anderson, P.M., 1985. Late Quaternary Vegetational change in the Kotzebue Sound area, northwestern Alaska. Quaternary Research 24, 307–321.

Anderson, P.M., 1988b. Late Quaternary pollen records from the Kobuk And Noatak River drainages, northwerstern Alaska. Quaternary Research 29, 263–276.

Anderson, P.M., Brubaker, L.B., 1994. Vegetation history of north-central Alaska: a mapped summary of Late-Quaternary pollen data. Quaternary Science Reviews 13, 71–92.

Anderson, P.M., Bartlein, P.J., Brubaker, L.B., 1994. Late Quaternary history of tundra vegetation in northwestern Alaska. Quaternary Research 41, 306–315.

Ashley, G.M., Hamilton, T.D., 1993. Fluvial response to late Quaternary climatic fluctuations, central Kobuk Valley, northwestern Alaska. Journal of Sedimentary Petrology 63, 814–827.

Barber, V.A., Juday, G.P., Finney, B.P., 2000. Reduced growth of Alaskan white spruce in the twentieth century from temperature-induced drought stress. Nature 405, 668–673.

Bartlein, P.J., Anderson, K.H., Anderson, P.M., Edwards, M.E., Mock, C.J., Thompson, R.S., Webb, R.S., Webb III, T., Whitlock, C., 1998. Paleoclimate stimulations for North America over the past 21,000 years: Features of the stimulated climate and

comparisons with paleoenvironmental data. Quaternary Science Reviews 17, 549–585.
Bennett, K.D., 1994. Confidence intervals for age estimates and deposition times in late-Quaternary sediment sequences. The Holocene 4, 337–348.
Bradley, R.S., 2000. Past global changes and their significance for the future. Quaternary Science Reviews 19, 391–402.
Briffa, K.R., 2000. Annual climate variability in the Holocene: interpreting the message of ancient trees. Quaternary Science Reviews 19, 87–105.
Bullard, J.E., Thomas, D.S.G., Livingstone, I., Wiggs, G.F.S., 1997. Dunefield activity and interactions with climatic variability in the southwest Kalahari Desert. Earth Surface Processes and Landforms 22, 165–174.
Calkin, P.E., 1988. Holocene glaciation of Alaska (and adjoining Yukon Territory, Canada). Quaternary Science Reviews 7, 159–184.
Calkin, P.E., Kaufman, D.S., Przybyl, B.J., Whitford, W.B., Peck, B.J., 1998. Glacier regimes, periglacial landforms, and Holocene climate change in the Kigluaik Mountains, Seward Peninsula, Alaska, USA. Arctic and Alpine Research 30, 154–165.
Carter, L.D., 1981. A pleistocene sand sea on the Alaskan arctic coastal Plain. Science 211, 381–383.
Chen, P.-Y., 1977. Table of key lines in X-ray powder diffraction patterns of minerals in clays and associated rocks. Indiana Geological Survey Occasional Paper 21, Indiana Department of Natural Resources, Bloomington, IN, 67pp.
Clark, M.L., Rendell, H.M., 1998. Climate-change impacts on sand supply and the formation of sand dunes in the south-west USA. Journal of Arid Environments 39, 517–531.
Cooke, R., Warren, A., Goudie, A., 1993. Desert Geomorphology. University College London Press, London.
Cooper, W.S., 1967. Coastal dunes of California. Geological Society of America Memoir 104, 131pp.
Cox, G.W., Lawrence, W.T., 1983. Cemented horizon in Alaskan sand dunes. American Journal of Science 283, 369–373.
Cwynar, L.C., Spear, R.W., 1991. Reversion of forest to tundra in the central Yukon. Ecology 72, 202–212.
Cwynar, L.C., Spear, R.W., 1995. Paleovegetation and paleoclimatic changes in the Yukon at 6 KA BP. Géographie physique et Quaternaire 49, 29–35.
D'Arrigo, R.D., Jacoby Jr., G.C., 1995. Dendroclimatic evidence from northern North America. In: Bradley, R.S., Jones, P.D. (Eds.), Climate Since A.D. 1500. Routledge, London, pp. 296–311.
David, P.P., 1981. Stabilized dune ridges in northern Saskatchewan. Canadian Journal of Earth Sciences 18, 286–310.
Dean, W.E., 1974. Determination of carbonate and organic matter in calcareous sediments and sedimentary rocks by loss on ignition: comparison with other methods. Journal of Sedimentary Petrology 44, 242–248.
Dean, W.E., 1999. The carbon cycle and biogeochemical dynamics in lake sediments. Journal of Paleolimnology 21, 375–393.
DeHarpporte, D., 1983. Northwest, North Central, and Alaska Wind Atlas. Van Nostrand Reinhold Company, New York.
Dijkmans, J.W.A., Koster, E.A., 1990. Morphological development of dunes in a subarctic environment, central Kobuk valley, northwestern Alaska. Geografiska Annaler 72A, 93–109.
Dijkmans, J.W.A., Galloway, J.P., Koster, E.A., 1988. Grain-size and mineralogy of eolian and fluvial sediments in the central Kobuk valley, northwestern Alaska. United States Geological Survey Open-File Report 88-369, 21pp.
Dijkmans, J.W.A., Koster, E.A., Galloway, J.P., Mook, W.G., 1986. Charactersistics and origin of calcretes in a subarctic environment, Great Kobuk Sand Dunes, northwestern Alaska, U.S.A. Arctic and Alpine Research 18, 377–387.
Edwards, M.E., Barker Jr., E.D., 1994. Climate and vegetation in northeastern Alaska 18,000 yr B.P.-present. Palaeogeography, Palaeoclimatology, Palaeoecology 109, 127–135.
Ellis, J.M., Calkin, P.E., 1984. Chronology of Holocene glaciation, central Brooks Range. Geological Society of America Bulletin 95, 897–912.
Fernald, A.T., 1964. Surficial geology of the central Kobuk River valley, northwestern Alaska. United States Geological Survey Bulletin 1181-K, k1–k31.
Ferrians Jr., O.J., 1994. Permafrost in Alaska. In: Plafker, G., Berg, H.C. (Eds.), The Geology of Alaska. Geological Society of America, Boulder, CO, pp. 845–854.
Filion, L., 1984. A relationship between dunes, fire and climate recorded in the Holocene deposits of Quebec. Nature 309, 543–546.
Filion, L., 1987. Holocene development of parabolic dunes in the central St. Lawrence, lowland Quebec. Quaternary Research 28, 196–209.
Galloway, J.P., Huebner, M., Lipkin, R., Dijkmans, J.W.A., 1990. Early Holocene calcretes from the subarctic active Nogahabara dune field, northern Alaska. United States Geological Survey Bulletin 1999, 100–109.
Galloway, J.P., Carter, L.D., 1993. Late holocene longitudinal and parabolic dunes in northern Alaska: preliminary interpretations of age and paleoclimatic significance. United States Geological Survey Bulletin 2068, 3–11.
Hamilton, T.D., 1984. Surficial geologic map of the Ambler River quadrangle Alaska. United States Geological Survey Miscellaneous Field Studies Map MF-1678, scale 1:250,000, 1 sheet.
Hamilton, T.D., Ashley, G.M., 1993. Epiguruk: a late quaternary environmental record from northwestern Alaska. Geological Society of America Bulletin 105, 583–602.
Hamilton, T.D., Galloway, J.P., Koster, E.A., 1987. Late Wisconsin eolian activity and related alluvium, central Kobuk valley. United States Geological Survey Circular 1016, 39–43.
Hare, F.K., Hay, J.E., 1974. The climate of Canada and Alaska. In: Bryson, R.A., Hare, F.K. (Eds.), World Survey of Climatology. Vol. 11, Climates of North America, Elsevier Scientific, New York, pp. 49-192.
Hartman, C.W., Johnson, P.R., 1984. Environmental Atlas of Alaska. Institute of Water Resources and Engineering Experiment Station, University of Alaska, Fairbanks, Alaska, 95pp.
Hopkins, D.M., 1982. Aspects of the paleogeography of Beringia during the late Pleistocene. In: Hopkins, D.M., Matthews, J.V., Schweger, C.E., Young, S.B. (Eds.), Paleoecology of Beringia. New York, Academic Press, pp. 3–28.
Hu, F.S., Brubaker, L.B., Anderson, P.M., 1996. Boreal ecosystem development in the northwestern Alaska Range since 11,000 yr B.P. Quaternary Research 45, 188–201.
Hu, F.S., Ito, E., Brubaker, L.B., Anderson, P.M., 1998. Ostracode geochemical record of Holocene climatic change and implications for vegetational response in the northwestern Alaska Range. Quaternary Research 49, 86–95.
Hunter, R.E., 1977. Basic types of stratification in small eolian dunes. Sedimentology 24, 361–387.
Jaboby, G.C., Workman, K.W., D'Arrigo, R.D., 1999. Laki eruption of 1783, tree rings, and disaster for the northwest Alaska Inuit. Quaternary Science Reviews 18, 1365–1371.
Kelts, K., Hsü, K.J., 1978. Freshwater carbonate sedimentation. In: Lerman, A. (Ed.), Lakes: Chemistry, Geology, Physics. Springer, New York, pp. 295–323.
Kocurek, G., 1998. Aeolian system response to external forcing factors — a sequence stratigraphic view of the Saharan region. In: Alsharan, A., Glennie, K.W., Wintle, G.L., St. C. Kendall, C.G. (Eds.), Quaternary Deserts and Climate Change, A.A. Balkema, Rotterdam, The Netherlands. pp. 327–337.

Kocurek, G., Lancaster, N., 1999. Aeolian system sediment state: theory and Mojave Desert Kelso dune field example. Sedimentology 46, 505–515.

Kolstrup, E., Jorgensen, J.B., 1982. Older and younger coversand in southern Jutland (Denmark). Bulletin of the Geological Society of Denmark 30, 71–77.

Koster, E.A., Dijkmans, J.W.A., 1988. Niveo-aeolian deposits and denivation forms, with special reference to the Great Kobuk Sand Dunes, northwestern Alaska. Earth Surface Processes and Landforms 13, 153–170.

Koster, E.A., Galloway, J.P., Mook, W.G., 1986. Characteristics and origin of calcretes in a subarctic environment, Great Kobuk Sand Dunes, northwestern Alaska, USA. Arctic and Alpine Research 18, 377–387.

Koster, E.A., Galloway, J.P., Pronk, T., 1984. Photo-interpretation map of surficial deposits and landforms of the Nogahabara Sand Dunes and part of the Koyukuk lowland, Alaska, United States Geological Survey Open-File Report 84–10.

Krishnaswami, S., Lai, D., 1978. Radionuclide limnochronology. In: Lerman, A. (Ed.), Lakes: Chemistry, Geology, Physics. Springer, New York, pp. 155–177.

Kuhry-Helmens, K.F., Koster, E.A., Galloway, J.P., 1985. Photo-interpretation map of surficial deposits and landforms of the Kobuk sand dunes and part of the Kobuk lowland, Alaska. United States Geological Survey Open File Report 85–242.

Lancaster, N., 1995. Geomorphology of Desert Dunes. Routledge, London.

Lea, P.D., 1990. Pleistocene periglacial eolian deposits in southwestern Alaska: sedimentary facies and depositional processes. Journal of Sedimentary Petrology 60, 582–591.

Lea, P.D., Waythomas, C.F., 1990. Late-Pleistocene eolian sand sheets in Alaska. Quaternary Research 34, 269–281.

Leslie, L.D., 1989. Alaska climate summaries: a compilation of long-term means and extremes at 478 Alaskan stations. Arctic Environmental Information and Data Center. University of Alaska Anchorage, Anchorage, Alaska, 478pp.

Loope, D.B., Swinehart, J.B., Mason, J.P., 1995. Dune-dammed paleovalleys of the Nebraska Sand Hills: intrinsic versus climatic controls on the accumulation of lake and marsh sediments. Geological Society of America Bulletin 107, 396–406.

Madole, R.F., 1994. Stratigraphic evidence of desertification in the west-central Great Plains within the past 1000 yr. Geology 22, 483–486.

Mason, O.K., Jordan, J.W., 1993. Heightened North Pacific storminess during synchronous late holocene erosion of northwest Alaska beach ridges. Quaternary Research 40, 55–69.

Mason, O.K., Jordan, J.W., Plug, L., 1995. Late Holocene storm and sea-level history in the Chukchi Sea. In: Finkl, C.W. (Ed.), Holocene Cycles: Climate, Sea Levels, and Sedimentation. Journal of Coastal Research Special Publication Number 17, pp. 173–180.

Maxwell, B., 1996. Recent climate patterns in the Arctic. In: Oechel, W.C., Callaghan, T., Gilmanov, T., Holten, J.I., Maxwell, B., Molau, U., Sveinbjornsson, B. (Eds.), Global Change and Arctic Terrestrial Ecosystems. Springer, New York, pp. 21–46.

McKenna-Neuman, C., 1993. A review of aeolian transport processes in cold environments. Progress in Physical Geography 17, 137–155.

McKenna-Neuman, C., Gilbert, R., 1986. Aeolian processes and landforms in glaciofluvial environments of southeastern Baffin Island N.W.T., Canada. In: Nickling, W.G. (Ed.), Aeolian Geomorphology. Proceedings of the 17th Annual Binghamton Geomorphology Symposium. Allen and Unwin, Boston, pp. 220–236.

Mock, C.J., Bartlein, P.J., Anderson, P.M., 1998. Atmospheric circulation patterns and spatial climatic variability in Beringia. International Journal of Climatology 18, 1085–1104.

Moritz, R.E., 1979. Synoptic Climatology of the Beaufort Sea Coast of Alaska. Occasional Paper Number 30, Institute of Arctic and Alpine Research, University of Colorado, Boulder, CO.

Moser, K.A., MacDonald, G.M., 1990. Holocene vegetation change at treeline north of Yellowknife, Northwest Territories, Canada. Quaternary Research 34, 227–239.

Muhs, D.R., Holliday, V.T., 1995. Evidence of active dune sand on the Great Plains in the 19th century from accounts of early explorers. Quaternary Research 43, 198–208.

Muhs, D.R., Maat, P.B., 1993. The potential response of eolian sands to greenhouse warming and precipitation reduction on the Great Plains of the USA. Journal of Arid Environments 25, 351–361.

Muhs, D.R., Stafford, T.W., Cowherd, S.D., Mahan, S.A., Kihl, R., Maat, P.B., Bush, C.A., Hehring, J., 1996. Origin of the late Quaternary dune fields of northeastern Colorado. Geomorphology 17, 129–149.

Muhs, D.R., Stafford Jr., T.W., Swinehart, J.B., Cowherd, S.D., Mahan, S.A., Bush, C.A., Madole, R.F., Maat, P.B., 1997. Late Holocene eolian activity in the mineralogically mature Nebraska Sand Hills. Quaternary Research 48, 162–176.

Murton, J.B., Worsley, P., Gozdzik, J., 2000. Sand veins and wedges in cold aeolian environments. Quaternary Science Reviews 19, 899–922.

Newman, J.E., Branton, C.I., 1972. Annual water balance and agricultural development in Alaska. Ecology 53, 513–519.

O'Connor, P.W., Thomas, D.S.G., 1999. The timing and environmental significance of late quaternary linear dune development in western Zambia. Quaternary Research 52, 44–55.

Overpeck, J., et al., 1997. Arctic environmental change of the last four centuries. Science 278, 1251–1256.

Patric, J.H., Black, P.E., 1968. Potential evaporation and climate in Alaska by Thornthwaite's classification. United States Department of Agriculture Forest Service Research Paper PNW-71. Pacific Northwest Forest and Range Experimental Station, Institute of Northern Forestry, Juneau, AL.

Pienitz, R., Smol, J.P., MacDonald, G.M., 1999. Paleoliminological reconstruction of holocene climatic trends from two boreal treeline lakes, Northwest Territories, Canada. Arctic, Antarctic, and Alpine Research 31, 82–93.

Pienitz, R., Smol, J., Last, W.M., Leavitt, P.R., Cumming, B.F., 2000. Multi-proxy Holocene paleoclimatic record from a saline lake in the Canadian subarctic. The Holocene, in press.

PRISM, 2000. Parameter-elevation regressions on independent slopes models for Alaska. http://www. ocs. orst.edu/prism/stat_products/ak_maps. html. Oregon Climate Service, 326 Strand Agriculture Hall, Oregon State University, Corvallis, OR97331.

Rabus, B.T., Echelmeyer, K.A., 1998. The mass balance of McCall Glacier, Brooks Range, Alaska; its regional relevance and implications for climate change in the Arctic. Journal of Glaciology 44, 333–351.

Racine, C.H., 1976. Flora and vegetation. In: Melchior, H.R., (Ed.), Biological Survey of the Proposed Kobuk Valley National Monument. Final Report to the United States National Park Service, Alaska Cooperative Park Studies Unit, University of Alaska, Fairbanks, Alaska. pp. 39–139,

Raup, H.M., Argus, G.W., 1982. The Lake Athabasca sand dunes of northern Saskatchewan and Alberta, Canada. I. The land and vegetation. National Museum of Natural Sciences Publications in Botany, No. 12, 96pp. National Museums of Canada, Ottawa, Canada.

Seppällä, M., 1995. Deflation and redeposition of sand dunes in Finnish Lapland. Quaternary Science Reviews 14, 799–809.

Stuiver, M., et al., 1998. INTCAL98 radiocarbon age calibration, 24,000–0 cal BP: Radiocabon 40, 1041–1083.

Tchakerian, V.P., 1994. Paleoclimatic interpretation from desert dunes and sediments. In: Abrahams, A.D., Parsons, A.J. (Eds.), Geomorphology of Desert Environments. Chapman and Hall, London, pp. 631–643.

van Vliet-Lanoë, B., Seppälä, M., Käyhkö, J., 1993. Dune dynamics and cryoturbation features controlled by Holocene water level change, Hietatievat, Finnish Lapland. Geologie en Mijnbouw 72, 211–224.

Wolfe, S.A., Muhs, D.R., David, P.P., McGeehin, J.P., 2000. Chronology and geochemistry of late holocene eolian deposits in the Brandon Sand Hills, Manitoba, Canada. Quaternary International 67, 61–74.

Wright, H.E., Mann, D.H., Glaser, P.H., 1984. Piston corers for peat and lake sediments. Ecology 65, 657–659.

Young, S.B., Racine, C.H., 1977. Vegetational and floristic analysis and discussion of the Quaternary environment of the Kobuk valley. Report to the United States National Park Service, Center for Northern Studies, Wolcott, VT, 47pp.